GM-CSF Controls Nonlymphoid Tissue Dendritic Cell Homeostasis but Is Dispensable for the Differentiation of Inflammatory Dendritic Cells

Published in final edited form as:
Immunity. 2012 June 29; 36(6): 1031–1046. doi:10.1016/j.immuni.2012.03.027.

GM-CSF Controls Nonlymphoid Tissue Dendritic Cell Homeostasis but Is Dispensable for the Differentiation of Inflammatory Dendritic Cells

Melanie Greter[1,2,8], **Julie Helft**[1,2], **Andrew Chow**[1,2], **Daigo Hashimoto**[1,2], **Arthur Mortha**[1,2], **Judith Agudo-Cantero**[2,3], **Milena Bogunovic**[1,2], **Emmanuel L. Gautier**[2,4], **Jennifer Miller**[1,2], **Marylene Leboeuf**[1,2], **Geming Lu**[2,5], **Costica Aloman**[5], **Brian D. Brown**[2,3,6], **Jeffrey W. Pollard**[7], **Huabao Xiong**[2,5,6], **Gwendalyn J. Randolph**[2,4], **Jerry E. Chipuk**[1,6], **Paul S. Frenette**[7], and **Miriam Merad**[1,2,6,*]

[1]Department of Oncological Sciences, Mount Sinai School of Medicine, New York, NY 10029, USA

[2]The Immunology Institute, Mount Sinai School of Medicine, New York, NY 10029, USA

[3]The Genomic Institute, Mount Sinai School of Medicine, New York, NY 10029, USA

[4]Department of Developmental and Regenerative Biology, Mount Sinai School of Medicine, New York, NY 10029, USA

[5]Department of Medicine, Mount Sinai School of Medicine, New York, NY 10029, USA

[6]Tisch Cancer Institute, Mount Sinai School of Medicine, New York, NY 10029, USA

[7]Albert Einstein College of Medicine, 1300 Morris Park Avenue, Bronx, New York, NY 10461, USA

SUMMARY

GM-CSF (Csf-2) is a critical cytokine for the in vitro generation of dendritic cells (DCs) and is thought to control the development of inflammatory DCs and resident $CD103^+$ DCs in some tissues. Here we showed that in contrast to the current understanding, Csf-2 receptor acts in the steady state to promote the survival and homeostasis of nonlymphoid tissue-resident $CD103^+$ and $CD11b^+$ DCs. Absence of Csf-2 receptor on lung DCs abrogated the induction of $CD8^+$ T cell immunity after immunization with particulate antigens. In contrast, Csf-2 receptor was dispensable for the differentiation and innate function of inflammatory DCs during acute injuries. Instead, inflammatory DCs required Csf-1 receptor for their development. Thus, Csf-2 is important in vaccine-induced $CD8^+$ T cell immunity through the regulation of nonlymphoid tissue DC homeostasis rather than control of inflammatory DCs in vivo.

INTRODUCTION

Dendritic cells (DCs) are professional antigen-presenting cells and key regulators of innate and adaptive immune responses. Tissue-resident DCs refer to DCs other than plasmacytoid DCs that populate the normal noninflamed tissues. In mice, tissue-resident DCs consist of

*Correspondence: miriam.merad@mssm.edu.
[8]Present address: Institute of Experimental Immunology, Neuroimmunology, University of Zurich, 8057 Zurich, Switzerland

SUPPLEMENTAL INFORMATION

Supplemental Information includes seven figures and can be found with this article online at doi:10.1016/j.immuni.2012.03.027.

two phenotypically and developmentally distinct subsets that include the $CD8^+CD103^+$ DCs and the $CD11b^+$ DC subsets (Hashimoto et al., 2011b; Heath and Carbone, 2009). The $CD8^+CD103^+$ DCs share a common origin, phenotype, and function. They derive from DC-restricted precursors independent of monocytes (Bogunovic et al., 2009; Ginhoux et al., 2009; Liu et al., 2009; Naik et al., 2007; Onai et al., 2007; Varol et al., 2009) and are dependent on Flt3 ligand (Flt3L) and on the transcription factors Batf3, IRF8, and Id2 for their development (Edelson et al., 2010; Ginhoux et al., 2009; Hashimoto et al., 2011b; Hildner et al., 2008). Phenotypically, they lack the integrin CD11b and the macrophage markers F4/80 and SIRPα (CD172a) and they express the integrin CD103 in nonlymphoid tissues, whereas in lymphoid organs they express the lymphoid marker CD8 (Edelson et al., 2010; Ginhoux et al., 2009; Hashimoto et al., 2011b; Hildner et al., 2008). In contrast, $CD11b^+$ DCs are more heterogeneous and include DCs that arise from DC-restricted precursors in a Flt3L-dependent manner, but also DCs that arise from circulating monocytes and macrophage-colony stimulating factor (M-CSF, Csf-1) receptor (Csf-1r) do not require Batf3, Id2, and IRF8 for their development (Edelson et al., 2010; Ginhoux et al., 2009; Hashimoto et al., 2011b; Hildner et al., 2008). In addition to tissue-resident DCs, tissue-draining lymph nodes (LNs) also contain nonlymphoid tissue $CD103^+$ DCs and $CD11b^+$ DCs that have migrated from the drained tissue, also called “tissue migratory cDCs” (Randolph et al., 2005).

In the inflamed setting, however, a distinct population of DCs is transiently formed and accumulates in injured tissues in response to microbial or inflammatory stimuli and disappears once the inflammation resolves. Inflammatory DCs are thought to derive from circulating $Ly6C^{hi}$ monocytes and are best characterized by the expression of Ly6C, high expression of the integrin CD11b, and intermediate levels of the integrin CD11c (Domínguez and Ardavín, 2010). One of the best examples of inflammatory DCs are TNF-α- and iNOS-producing DCs (TipDCs) (Serbina et al., 2003) that accumulate in the spleen of mice infected with *Listeria monocytogenes* (*L. monocytogenes*). TipDCs and inflammatory DCs have also been described in other inflammatory diseases (Domínguez and Ardavín, 2010) and participate in the control of infections (Aldridge et al., 2009; León and Ardavín, 2008; Rydström and Wick, 2007; Serbina et al., 2003).

Granulocyte-macrophage colony stimulating factor (GM-CSF, Csf-2) is a hematopoietic growth factor that controls the differentiation of the myeloid lineage (Metcalf, 2008). In addition to its effects on hematopoietic progenitors, Csf-2 can also modulate the function of mature hematopoietic cells (Metcalf, 2008). For example, in the lung, Csf-2 is essential to promote surfactant clearance by alveolar macrophages, and deletion of Csf-2 (Dranoff et al., 1994; Stanley et al., 1994) or Csf-2 receptor (Csf-2r) (Nishinakamura et al., 1995) leads to alveolar proteinosis because of the accumulation of lipoproteinaceous material in lung alveoli (Trapnell et al., 2003). The pivotal role for Csf-2 in DC development was first identified by in vitro studies. In these studies, Csf-2 was required to promote the differentiation of mouse and human hematopoietic progenitors and human circulating monocytes into cells that resemble mouse splenic DCs (Caux et al., 1996; Inaba et al., 1992; Sallusto and Lanzavecchia, 1994). Csf-2 remains to date a key cytokine to generate DC-based vaccines for clinical use (Banchereau and Palucka, 2005). Therefore, it came as a surprise that mice lacking Csf-2 or its receptor displayed only minor impairment in the development of spleen and lymph node (LN) DCs (Vremec et al., 1997). Subsequent studies showing that Csf-2 is increased in the serum of inflamed mice, together with data suggesting that adoptively transferred monocytes differentiate into DCs mainly in the inflamed spleen, led to the current dogma that Csf-2 controls monocyte-derived DC differentiation in vivo (Naik et al., 2006; Shortman and Naik, 2007). Results from our laboratory revealed that absence of Csf-2r impaired the development of a specific lamina propria DC population (Bogunovic et al., 2009). A subsequent study revealed that Csf-2 also controls the

development of dermal CD103$^+$ DCs (King et al., 2010), prompting us to revisit the role of Csf-2 and its receptor in the control of the DC lineage.

Our data revealed that Csf-2r signaling is required for the development of nonlymphoid tissue-resident DCs in the steady state and for the induction of CD8$^+$ T cell immunity against particulate antigens. We also found that in contrast to the current understanding, inflammatory DCs that accumulate in injured tissues develop independently of Csf-2r signaling and identified Csf-1r as a key molecule for the development of inflammatory DCs.

RESULTS

DCs Have High Csf-2r Expression in the Steady State

To determine the role of Csf-2 in DC development in the steady state, we first examined the expression profile of the Csf-2r among lymphoid and nonlymphoid tissue DCs in normal noninflamed conditions. Csf-2 binds specifically to the Csf-2r, a heterodimer composed of a cytokine-specific α chain (Csf-2ra, *Csf2ra*) and a common signaling β chain (βc, Csf-2rb, *Csf2rb*) that is shared with the receptors for IL-3 (IL-3r) and IL-5 (IL-5r) (Martinez-Moczygemba and Huston, 2003). In mice, IL-3r also possesses a second β subunit called Csf-2rb2 (*Csf2rb2*), which together with IL-3r-specific α chain is sufficient to drive IL-3 signaling in the absence of Csf-2rb (Robb et al., 1995).

Expression array analysis of tissue-resident and migratory DC subsets in nonlymphoid and lymphoid tissues revealed that all DC subsets expressed high amounts of *Csf2ra* and *Csf2rb* transcript (Figure 1A; Figure S1A available online). By using flow cytometry analysis, we confirmed that Csf-2rb was also highly expressed on lymphoid and nonlymphoid tissue DCs (Figure 1B). Splenic CD4$^+$ and CD8$^+$ T cells that lack Csf-2rb (Morrissey et al., 1987; Sonderegger et al., 2008) and neutrophils that express Csf-2rb were used as controls. In contrast, in the steady state, nonlymphoid tissue DCs expressed low IL-3r- and IL-5r-specific α chains (IL-3ra and IL-5ra, respectively) (Figures 1A and 1C).

Csf-2r Controls Nonlymphoid Tissue DC Homeostasis In Vivo

To further establish the role of Csf-2 in DC development in the steady state, we examined whether lymphoid tissue CD8$^+$ and CD11b$^+$ and nonlymphoid tissue CD103$^+$ and CD11b$^+$ DC populations were affected in Csf-2r-deficient (*Csf2rb*$^{-/-}$*Csf2rb2*$^{-/-}$) mice that lack the common β subunit (*Csf2rb*) and the IL-3r unique β subunit (*Csf2rb2*). We found that *Csf2rb*$^{-/-}$*Csf2rb2*$^{-/-}$ mice have much lower numbers of CD103$^+$ DCs in the lung, lung-draining LNs, and lamina propria compared to wild-type (WT) mice (Figures 1D and S1). Consistent with prior studies (King et al., 2010), CD103$^+$ DCs were also strongly reduced in the dermis and skin-draining LNs of *Csf2rb*$^{-/-}$*Csf2rb2*$^{-/-}$ mice, whereas spleen, LN-resident DCs, and epidermal Langerhans cells (LCs) developed normally in the absence of Csf-2r (Bogunovic et al., 2009; Vremec et al., 1997; data not shown). CD11b$^+$ DCs were not affected in *Csf2rb*$^{-/-}$*Csf2rb2*$^{-/-}$ mice except in the lamina propria, where CD11b$^+$CD103$^+$ DCs were reduced (Figure 1D).

Csf-2 Controls Nonlymphoid Tissue DC Homeostasis In Vivo

As shown above, tissue DCs express no IL-5ra (Figures 1A–1C). Therefore, DC defects observed in *Csf2rb*$^{-/-}$*Csf2rb2*$^{-/-}$ mice are probably independent of IL-5, but combined defects in Csf-2 and IL-3 signaling could potentially contribute to the DC phenotype observed in these mice. To examine the contribution of Csf-2 and IL-3 to DC homeostasis, we analyzed tissue DCs in *Csf2rb*$^{-/-}$ mice, which have intact Csf-2rb2 chain and can therefore respond to IL-3 stimulation (Robb et al., 1995). Nonlymphoid tissue DCs were similarly reduced in *Csf2rb*$^{-/-}$ mice compared to *Csf2rb*$^{-/-}$*Csf2rb2*$^{-/-}$ mice, establishing that

IL-3 is dispensable for DC homeostasis in vivo (Figure S1B). Similar to *Csf2rb*$^{-/-}$ mice, *Csf2*$^{-/-}$ mice had a strong reduction of lung- and skin-resident CD103^{+} DCs as well as migratory CD103^{+} DCs in the lung-draining and skin-draining LNs (Figure 1E) and also displayed reduced numbers of lung CD11b^{+} DCs, dermal CD11b^{+} DCs, and CD103^{+}CD11b^{+} DCs in the lamina propria and mesenteric LNs, establishing that Csf-2 is required to maintain DC homeostasis in nonlymphoid tissues in vivo. To assess the source of Csf-2 required to support DC homeostasis, we generated WT→*Csf2*$^{-/-}$ bone marrow (BM) chimeric mice as well as *Csf2*$^{-/-}$→WT BM chimeras. We found that tissue CD103^{+} and CD11b^{+} DCs were reduced both in WT→*Csf2*$^{-/-}$ and *Csf2*$^{-/-}$→WT BM chimeric mice, suggesting that Csf-2 produced by radiosensitive hematopoietic cells and radio-resistant cells contributes to DC homeostasis (Figure S2).

Csf-2 regulates CD103 expression on DCs (Zhan et al., 2011), which prompted us to determine whether CD103^{+} DC defects observed in *Csf2rb*$^{-/-}$*Csf2rb2*$^{-/-}$ mice reflected a true reduction of CD103^{+} DCs or only a modulation of CD103 expression by this cell population. Therefore, we assessed the reduction of DCs using surrogate markers of CD103^{+} DCs, such as the marker CD24 and lack of expression of CD11b (Figure S1). Importantly, we found that nonlymphoid tissue CD24^{+}CD11b^{-} DCs were also reduced in *Csf2*$^{-/-}$ mice (Figure 1E) and *Csf2rb*$^{-/-}$ mice (Figure S1B), suggesting that absence of Csf-2r affected not only CD103 expression but also CD103^{+} DC homeostasis in vivo.

Csf-2r Plays a Cell-Intrinsic Role in DC Homeostasis

To examine whether Csf-2r regulation of tissue DC homeostasis was cell intrinsic, we generated mixed BM chimeric mice with a 1:1 mixture of CD45.1^{+} WT:CD45.2^{+}*Csf2rb*$^{-/-}$*Csf2rb2*$^{-/-}$ or CD45.1^{+} WT:CD45.2^{+} WT BM cells. Two months after reconstitution, we found that CD45.2^{+}*Csf2rb*$^{-/-}$*Csf2rb2*$^{-/-}$CD103^{+} DCs were strongly reduced in the lung, skin, liver, and kidney in comparison to WT CD103^{+} DCs in the same animal and compared to CD103^{+} DCs in WT BM chimeric mice (Figures 2A–2D). Importantly, CD45.2^{+}*Csf2rb*$^{-/-}$*Csf2rb2*$^{-/-}$CD11b^{+} DCs were also reduced in the lung, lung-draining LN, dermis, skin-draining LN, lamina propria, and mesenteric LN, suggesting that Csf-2r also regulates cell intrinsically the homeostasis of the CD11b^{+} DC subset in vivo.

Consistent with our finding in mutant mice, *Csf2rb*$^{-/-}$ *Csf2rb2*$^{-/-}$CD24^{+}CD11b^{-} DCs in mixed BM chimeric animals were strongly reduced in the lung and lung-draining LN compared to WT DCs, and CD103 expression was further reduced on the remaining *Csf2rb*$^{-/-}$*Csf2rb2*$^{-/-}$CD24^{+}CD11b^{-} DCs (Figure S3C). The numbers of CD24^{+}*Csf2rb*$^{-/-}$*Csf2rb2*$^{-/-}$ kidney DCs were only slightly decreased although they exhibited a complete downregulation of CD103 (Figure 2D). These data indicate that although Csf-2 ubiquitously regulates the expression of CD103, the impact of Csf-2 on DC homeostasis is tissue specific. Consistent with our findings in *Csf2rb*$^{-/-}$ *Csf2rb2*$^{-/-}$ mice, lymphoid tissue-resident DCs were not affected in mixed BM chimeric mice (Figure S3A). In addition, *Csf2rb*$^{-/-}$ BM chimeric mice cells displayed similar tissue DC defects (Figure 2E) as compared to *Csf2rb*$^{-/-}$*Csf2rb2*$^{-/-}$ chimeric mice, indicating again that DC deficiency resulted from abrogated Csf-2 signaling rather than disrupted IL-3 signaling. Thus, Csf-2 produced by hematopoietic and stromal cells drives Csf-2r cell-intrinsic control of nonlymphoid tissueresident CD103^{+} and CD11b^{+} DC homeostasis in vivo.

Csf-2r Does Not Control the Commitment of Hematopoietic Progenitors into the DC Lineage In Vivo

Recent studies established that the earliest myeloid commitment to the DC lineage occurs at the macrophage and DC precursor (MDP) stage. MDP gives rise to monocytes and to the common DC precursor (CDP) that produces exclusively plasmacytoid DCs and preDCs, a

circulating DC-restricted progenitor that gives rise exclusively to DCs in both lymphoid and nonlymphoid tissue DCs (Bogunovic et al., 2009; Fogg et al., 2006; Ginhoux et al., 2009; Liu et al., 2009; Naik et al., 2007; Onai et al., 2007; Varol et al., 2007; Waskow et al., 2008).

To examine whether Csf-2 controls DC homeostasis in vivo through its ability to control DC progenitor commitment, we analyzed the expression of Csf-2rb, IL-3ra, and IL-5ra on MDPs, CDPs, and preDCs at the mRNA and protein levels by gene expression arrays and flow cytometry (Figures 3A and 3B). Bone marrow MDPs and CDPs and preDCs expressed Csf-2rb and IL-3ra but not IL-5ra, whereas preDCs in the spleen expressed Csf-2rb but not IL-3ra and IL-5ra.

Absence of Csf-2rb and Csf-2rb2 did not affect the development of MDPs, CDPs, and preDCs in mixed BM chimeric mice (Figures 3C–3E), suggesting that the DC deficiency observed in *Csf2rb*$^{-/-}$*Csf2rb2*$^{-/-}$ mice does not stem from a defect at the precursor level but rather results from either impaired differentiation or survival of mature DCs in nonlymphoid tissues.

Csf-2r Controls DC Survival in Nonlymphoid Tissues

Consistent with the hypothesis that Csf-2 acts on DCs locally in nonlymphoid tissues, we found that Csf-2 expression was much higher in nonlymphoid tissues in comparison to the spleen or sera of naive WT mice (Figure 4A). To address whether Csf-2 plays a prosurvival role on tissue DCs, we cultured purified total splenic DCs and CD103^{+} lung DCs overnight in the presence or absence of Csf-2 and measured the activation of Caspase-3 (cleaved Caspase-3), which is indicative of cellular apoptosis. Csf-2 addition to the culture medium resulted in reduced active Caspase-3 by DCs together with increased absolute cell numbers (Figures 4B and 4C), indicating that Csf-2 promoted DC survival in vitro.

To further explore the prosurvival role of Csf-2 in vivo, we analyzed WT and *Csf2rb*$^{-/-}$*Csf2rb2*$^{-/-}$ DCs isolated from the lung of mixed BM chimeric animals for survival defects. First, we labeled *Csf2rb*$^{-/-}$*Csf2rb2*$^{-/-}$ and WT DCs with Mitogreen to assess mitochondrial network integrity via live cell fluorescent microscopy. In parallel to promoting Caspase activation, mitochondria undergo marked fission as a result of apoptosis (Riedl and Salvesen, 2007; Youle and Karbowski, 2005) and therefore fragmentation of the mitochondrial network provides an excellent measure of survival defects (Karbowski et al., 2002; Martinou and Youle, 2011). We found that the majority of mitochondria displayed a fragmented phenotype with occasional swelling and perinuclear localization in *Csf2rb*$^{-/-}$*Csf2rb2*$^{-/-}$ DCs whereas the mitochondrial membrane appeared unaffected in WT DCs isolated from the lung of the same animal (Figure 4D).

WT and *Csf2rb*$^{-/-}$*Csf2rb2*$^{-/-}$ DCs isolated from mixed BM chimeras were also stained with cleaved Caspase-3 antibody. Consistent with the Mitogreen data, we found an increased number of cleaved Caspase-3^{+} DCs among *Csf2rb*$^{-/-}$*Csf2rb2*$^{-/-}$ DCs compared to WT DCs (Figure S4A), strongly suggesting that Csf-2r plays a key prosurvival role in nonlymphoid tissue DCs in vivo. To directly probe the prosurvival role of Csf-2 in DCs in vivo, we measured the number of Annexin-V^{+} apoptotic DCs among the DCs that populate the lung and intestine of *Csf2*$^{-/-}$ and WT mice. We found a significantly higher number of Annexin-V^{+}DAPI^{-} DCs in the lung of *Csf2*$^{-/-}$ mice and in the small intestine of *Csf2rb*$^{-/-}$*Csf2rb2*$^{-/-}$ mice compared to WT mice (Figures S4B–S4D). Altogether, these results strongly establish the key role played by Csf-2 and Csf-2r in promoting DC survival in nonlymphoid tissues in vivo.

Csf2rb$^{-/-}$Csf2rb2$^{-/-}$ Mice Cannot Mount Efficient Antigen-Specific CD8^{+} T Cell Immunity upon Immunization with Particulate Antigens In Vivo

To determine whether the defect in nonlymphoid tissue DC development observed in *Csf2rb*$^{-/-}$*Csf2rb2*$^{-/-}$ mice would affect the cross-priming of antigen-specific CD8^{+} T cells upon immunization with particulate antigens, WT and *Csf2rb*$^{-/-}$*Csf2rb2*$^{-/-}$ mice were injected intratracheally (i.t.) with the adjuvant poly(I:C) together with latex beads coated with the model antigen ovalbumin (OVA) (Jakubzick et al., 2008). Seven days after immunization, we found that *Csf2rb*$^{-/-}$*Csf2rb2*$^{-/-}$ mice were unable to mount OVA-specific CD8^{+} T cell immunity compared to WT mice (Figure 4E). However, because *Csf2rb*$^{-/-}$*Csf2rb2*$^{-/-}$ mice also develop lung alveolar proteinosis secondary to defects in surfactant catabolism by alveolar macrophages (Nishinakamura et al., 1995) that may compromise T cell immune responses, we examined whether similar T cell priming defects also arise in *Csf2rb*$^{-/-}$*Csf2rb2*$^{-/-}$ BM chimeric mice that do not develop proteinosis, Strikingly, whereas WT BM chimeric mice mounted a robust OVA-specific CD8^{+} T cell response, *Csf2rb*$^{-/-}$*Csf2rb2*$^{-/-}$ BM chimeric mice were unable to mount OVA-specific CD8^{+} T cell immunity upon i.t. immunization with OVA-coated latex beads and poly(I:C) (Figure 4F). Defects in CD8^{+} T cells priming observed in *Csf2rb*$^{-/-}$*Csf2rb2*$^{-/-}$ BM chimeric mice were probably due to defective lung migratory CD103^{+}CD8^{-} DCs because lung CD103^{+}CD8^{-} DCs (Figure S5A) and lung migratory CD103^{+} CD8^{-} DCs were the main drivers of OT-I T cell proliferation in WT mice (Figure S5B). Because Csf-2r is expressed by DCs and not by T cells (Figure 1B; Morrissey et al., 1987; Sonderegger et al., 2008), these results suggest that Csf-2r controls the cross-priming of antigen-specific CD8^{+} T cells to particulate antigens through its role on nonlymphoid tissue migratory DCs.

Csf-2 Is Not Required for the Generation of Monocyte-Derived DCs in the Acute Inflamed State

Csf-2 is thought to control the differentiation of inflammatory DCs that accumulate in injured tissues (Shortman and Naik, 2007). To examine the regulation of inflammatory DC development, we used several distinct tissue infection and acute inflammatory models including intranasal (i.n.) infection with influenza A virus or *Streptococcus pneumoniae* (*S. pneumoniae*), oral *Salmonella* Typhimurium (*S.* Typhimurium) infection, systemic *Listeria monocytogenes* (*L. monocytogenes*) infection, or systemic lipopolysaccharide (LPS) injection. Inflammatory DCs that accumulated in influenza virus-infected lungs expressed MHCII, CD11c, CD11b, Ly6C, and Mac-3 (Figure 5A) as previously described (Serbina et al., 2003). Lung inflammatory DCs also expressed CD172a (Sirpα), F4/80, and CD24 (Figure 5A) as well as Csf-2r, but surprisingly they expressed higher Csf-1r levels and much lower Flt3 levels compared to lung tissue-resident DCs (Figure 5B).

To examine whether the development and function of inflammatory DCs was dependent on Csf-2r signaling, we analyzed the differentiation of inflammatory DCs in WT:*Csf2rb*$^{-/-}$*Csf2rb2*$^{-/-}$ mixed BM chimeric mice in inflamed tissues a few days after infection. Strikingly, a similar number of *Csf2rb*$^{-/-}$*Csf2rb2*$^{-/-}$ and WT DCs accumulated in influenza virus-infected lungs, *S. pneumonia* lungs (Figure 5C), LPS-exposed lungs and spleens (Figure 5D), and *S.* Typhimurium-infected lamina propria (Figure 5E). These results establish that blood-derived DCs can accumulate in acute inflamed tissues in the absence of Csf-2r signaling. Csf-2 also plays a pivotal role for the development of experimental autoimmune encephalomyelitis (EAE) (Codarri et al., 2011). However, consistent with our findings in microbial-induced injury models, similar numbers of *Csf2rb*$^{-/-}$ and WT inflammatory DCs were present in the CNS of mixed WT:*Csf2rb*$^{-/-}$ BM chimeras during the peak of disease in EAE mice (Figure S6).

To further assess whether monocytes differentiate into DCs in the absence of Csf-2r signaling, we transferred a 1:1 mixture of CD45.1$^+$ WT:CD45.2$^+$ *Csf2rb*$^{-/-}$*Csf2rb2*$^{-/-}$ monocytes into CD45.1$^+$CD45.2$^+$ F1 recipient mice 1 day after the recipient mice were infected i.n. with influenza virus. Two days after monocyte transfer, we measured the numbers of CD45.1$^+$ WT and CD45.2$^+$ *Csf2rb*$^{-/-}$*Csf2rb2*$^{-/-}$ monocyte-derived DCs in influenza virus-infected lungs and lung-draining LNs of F1 recipient animals (Figure 5F). We found that *Csf2rb*$^{-/-}$*Csf2rb2*$^{-/-}$ monocytes differentiate as efficiently as WT monocytes into inflammatory DCs in injured tissues (Figure 5F), suggesting that Csf-2r signaling does not control the differentiation of inflammatory monocyte-derived DCs in vivo.

Csf2rb$^{-/-}$Csf2rb2$^{-/-}$ Inflammatory DCs Have Normal Innate Immune Function

One of the hallmarks of inflammatory DCs is their ability to secrete TNF-α and/or iNOS (TipDCs), two molecules that control antimicrobial host defense (Serbina et al., 2008). To examine whether *Csf2rb*$^{-/-}$*Csf2rb2*$^{-/-}$ DCs were functionally impaired compared to WT DCs, we measured TNF-α and iNOS production of inflammatory *Csf2rb*$^{-/-}$*Csf2rb2*$^{-/-}$ and WT DCs isolated from influenza virus-infected lungs, *S. pneumonia*-infected lungs, and LPS-exposed lungs of mixed BM chimeric mice generated as described above. We found that *Csf2rb*$^{-/-}$*Csf2rb2*$^{-/-}$ inflammatory DCs were as potent as WT inflammatory DCs at producing TNF-α and iNOS in inflamed tissues (Figure 6A).

TipDCs have been shown to be most critical for the induction of early innate immune defense against *L. monocytogenes*, and *Ccr2*$^{-/-}$ mice that lack TipDCs die during the first few days after infection secondary to uncontrollable systemic *L. monocytogenes* spread (Kurihara et al., 1997). To examine whether the function of *Csf2rb*$^{-/-}$*Csf2rb2*$^{-/-}$ TipDCs was compromised, we compared the ability of WT and *Csf2rb*$^{-/-}$*Csf2rb2*$^{-/-}$ DCs to produce iNOS and to control bacterial burden upon systemic *L. monocytogenes* infection. *Ccr2*$^{-/-}$ mice were used as controls (Serbina et al., 2003). We found that a similar number of *Csf2rb*$^{-/-}$*Csf2rb2*$^{-/-}$ and WT TipDCs accumulated in the spleens of *L. monocytogenes*-infected animals (Figure 6B). *Csf2rb*$^{-/-}$*Csf2rb2*$^{-/-}$ TipDCs in the spleens of infected animals were as efficient as WT TipDCs at producing iNOS (Figures 6B and 6C) and *Csf2rb*$^{-/-}$*Csf2rb2*$^{-/-}$ mice were as efficient as WT mice at controlling the *L. monocytogenes* bacterial load in the spleen and liver during the first days of infection, which was consistent with the presence of TipDCs in these tissues (Figures 6C and 6D). In agreement with other reports, *Ccr2*$^{-/-}$ mice had a much higher bacterial burden in the spleen and liver. These results establish that TipDCs develop and function in vivo independently of Csf-2r signaling.

Csf-1r Controls the Differentiation of Inflammatory DCs

Csf-1 and its receptor (Csf-1r) is the primary regulator of the mononuclear phagocytic lineage. A null mutation of Csf-1r alters normal macrophage development (including osteoclast development leading to severe osteopetrosis) (Dai et al., 2002) and abrogates microglia development (Ginhoux et al., 2010) and the development of epidermal LCs (Ginhoux et al., 2006). Interestingly, we found that Csf-1r was expressed at high levels on inflammatory DCs (Figures 5B and 7A) and that Csf-1 was strongly increased in inflamed tissues (Figure 7B). These results prompted us to revisit the role of Csf-1r in the differentiation of monocyte-derived DCs in vivo.

We used two separate models to interfere with Csf-1r signaling in inflamed mice. First, we crossed Csf-1r-floxed (*Csf1r*$^{fl/fl}$) mice with tamoxifen-inducible Rosa26CreER (Cre$^+$) mice. Administration of tamoxifen to these mice leads to the excision of the *Csf1r*-floxed sequence resulting in a null allele (Li et al., 2006).

Interestingly, we found that tamoxifen injection eliminated Ly6C^{lo} circulating monocytes (Figure 7C) but did not affect the development of spleen- and LN-resident DCs and circulating Ly6C^{hi} monocytes in uninfected spleens (Figures S7A and S7B) nor did it affect the accumulation of Ly6C^{hi} monocytes in LPS-injured spleens (Figures 7D and S7B). In contrast, the number of inflammatory DCs that accumulated in LPS-treated spleens of Cre^{+} × *Csf1r*$^{fl/fl}$ tamoxifen-treated mice were reduced compared to control animals (Figures 7D and S7B). Similar results were obtained in influenza-infected mice (Figure 7G).

In a second model, we used a blocking monoclonal antibody to Csf-1r (AFS98) prior to treating the mice with LPS (Sudo et al., 1995). Consistent with the results obtained in *Csf1r*$^{fl/fl}$ mice, administration of Csf-1r antibody in LPS-treated mice strongly reduced Ly6C^{lo} monocytes without affecting the number of circulating Ly6C^{hi} monocytes as previously shown (Figure 7E; Hashimoto et al., 2011a; MacDonald et al., 2010). Administration of Csf-1r antibody did not affect the accumulation of circulating monocytes in inflamed tissues. In contrast, the number of inflammatory DCs that accumulated in LPS-treated spleens was dramatically reduced (Figure 7F) and they also displayed a lower expression of the costimulatory molecules CD80 and CD86 (Figure S7C). Altogether these results suggest that Csf-1r signaling, but not Csf-2r, may be critical for the differentiation of inflammatory DCs in vivo.

DISCUSSION

Csf-2 is a critical cytokine for the differentiation of monocytes and hematopoietic progenitors into DCs in vitro in mice and men (Caux et al., 1996; Inaba et al., 1992; Sallusto and Lanzavecchia, 1994). However, the exact role of Csf-2 in DC differentiation in vivo has remained an outstanding question in DC biology since the surprising discovery that *Csf2rb*$^{-/-}$ and *Csf2*$^{-/-}$ mice do not have impaired DC development in lymphoid organs (Vremec et al., 1997).

In this study we revisited the role of Csf-2 in DC differentiation in vivo. With mutant and mixed BM chimeric mice, we found that Csf-2 was absolutely critical for the homeostasis of nonlymphoid tissue DCs. Deletion of Csf-2, Csf-2rb, or both Csf-2rb and Csf-2rb2 profoundly affected the homeostasis of CD103^{+} and CD11b^{+} DCs in the lung, skin, and lamina propria, establishing that Csf-2 and not IL-3 was required for normal DC homeostasis. These results extend previous results from our laboratory showing that Csf-2r controls lamina propria DC homeostasis (Bogunovic et al., 2009) and more recent results showing that the formation or maintenance of dermal CD103^{+} DCs is dependent on Csf-2 (King et al., 2010). They are also consistent with the reported role for Csf-2 in the in vitro differentiation of CD103^{+} DCs from BM precursors (Sathe et al., 2011).

CD11b^{+} DCs as currently defined in nonlymphoid tissues are heterogeneous and probably contain a contaminating macrophage population that also expresses MHCII and CD11c in the steady state, as recently described in the gut (Bogunovic et al., 2009; Schulz et al., 2009; Varol et al., 2009). However, the lack of markers to accurately distinguish DCs from macrophages among MHCII^{+}CD11c^{+}CD11b^{+} cells in tissues other than the lamina propria (Hashimoto et al., 2011b) dilutes potential defects induced by the lack of Csf-2r and may explain the partial reduction of tissue-resident CD11b^{+} DCs compared to CD103^{+} DCs.

Importantly, *Csf2rb*$^{-/-}$*Csf2rb2*$^{-/-}$ mice and *Csf2rb*$^{-/-}$*Csf2rb2*$^{-/-}$ BM chimeric mice were unable to mount antigen-specific CD8^{+} effector T cells in the lung and the lung-draining LNs upon immunization with particulate antigens. These results are probably due to the strong reduction of lung CD103^{+} DCs that are most potent in inducing the cross-presentation of particulate antigens to CD8^{+} T cells (Hildner et al., 2008). In addition, it was recently

shown that Csf-2 controls DC cross-presentation and cross-priming function in vitro (Sathe et al., 2011). Csf-2-transduced tumor cells have been used to generate antitumor $CD8^+$ T cell immunity with some clinical success. The mechanisms that control the clinical potency of this vaccine are not clearly established but it is critical to examine whether these vaccines improve antitumor immunity, partly through their ability to promote the survival and/or the cross-presenting function of human equivalent $CD103^+$ DCs (Bachem et al., 2010; Crozat et al., 2010; Jongbloed et al., 2010; Poulin et al., 2010).

Our data also revealed that Csf-2 was produced by both hematopoietic and stromal cells in nonlymphoid tissues in the steady state and promoted the survival of tissue $CD103^+$ and $CD11b^+$ DCs by blocking the mitochondrial apoptosis pathway. In contrast, Csf-2 was expressed at low levels in lymphoid organs, and absence of Csf-2 or Csf-2r did not affect lymphoid tissue-resident DC homeostasis, which is consistent with prior data (Vremec et al., 1997). These results probably reflect the nonredundant role of Csf-2 in promoting DC survival in nonlymphoid tissue environment. In contrast, Csf-2 may be redundant in lymphoid organs, which harbor several hematopoietic cytokines such as Flt3L known to promote tissue DC homeostasis in vivo.

Inflammatory DCs are absent from normal tissues and accumulate only upon tissue injury. The exact mechanisms that control the development of inflammatory DCs remain to be defined but it is clear that inflammatory DCs derive from circulating bone marrow-derived precursors that probably include circulating $Ly6C^{hi}$ monocytes (Domínguez and Ardavín, 2010). The initial reports showing that Csf-2 is increased in the serum and lymphoid tissues of infected animals (Hamilton, 2008) led to the suggestion that Csf-2 controls the differentiation of inflammatory DCs (Shortman and Naik, 2007). Our results, however, do not support a critical role for Csf-2 in the differentiation of inflammatory DCs in acute models of inflammation. By using four different acute infection models, we found that *Csf2rb*$^{-/-}$*Csf2rb2*$^{-/-}$ DCs were phenotypically identical to and as potent as WT DCs at producing TNF-α and iNOS. Importantly, *Csf2rb*$^{-/-}$*Csf2rb2*$^{-/-}$ inflammatory DCs that arise in *L. monocytogenes*-infected spleens were as efficient as WT DCs at controlling the initial *L. monocytogenes* load of infected animals.

Because inflammatory DCs are thought to differentiate mainly from circulating $Ly6C^{hi}$ monocytes, we also examined whether adoptively transferred *Csf2rb*$^{-/-}$*Csf2rb2*$^{-/-}$ $Ly6C^{hi}$ monocytes can differentiate into DCs in vivo. Consistent with the data obtained in *Csf2rb*$^{-/-}$*Csf2rb2*$^{-/-}$ mice, adoptively transferred *Csf2rb*$^{-/-}$*Csf2rb2*$^{-/-}$ monocytes differentiated as efficiently as did WT monocytes into inflammatory DCs in influenza virus-infected lungs.

In contrast, Csf-1r blockade either through genetic or pharmacological means strongly impaired the accumulation of inflammatory DCs in influenza virus-infected lungs and in LPS-treated spleens, suggesting that Csf-1r signaling may promote the differentiation of monocytes into inflammatory DCs during acute tissue injuries. These results may help explain prior data showing that absence of Csf-1 alters the induction of *L. monocytogenes* immunity in vivo (Guleria and Pollard, 2001), although the exact role of Csf-1r in regulating the function of monocyte-derived DCs remains to be examined in detail.

These results also extend prior results showing that Csf-1r controls the differentiation of specific DC subsets such as epidermal LCs and kidney, lung, and gut $CD11b^+$ DCs (Bogunovic et al., 2009; Ginhoux et al., 2009; Hashimoto et al., 2011b). The exact role of Csf-1 in inflammatory DC homeostasis is currently being examined in the laboratory and may include a role in the differentiation, proliferation, and survival of DCs as shown for macrophages (Yu et al., 2008).

In sum, our results reveal that in contrast to the current dogma that suggests that Csf-2 mainly controls the development of inflammatory DCs in vivo, Csf-2 is a steady-state cytokine that controls the induction of $CD8^+$ T cell immunity to particulate antigens through the regulation of nonlymphoid tissue-resident DC survival and homeostasis. These results also reveal a role for Csf-1r in the differentiation of inflammatory DCs and provide a rationale for the development of clinical strategies using Csf-1r ligands to enhance innate antimicrobial immunity.

EXPERIMENTAL PROCEDURES

Mice

C57BL/6 (CD45.2) mice, C57BL/6 (CD45.1) mice, B6.129S1-Csf-2rb2tm1Cgb Csf-2rbtm1Clsc/J (*Csf2rb*$^{-/-}$*Csf2rb2*$^{-/-}$) mice, B6;129-Gt(ROSA)26Sortm1 (Rosa26-CreER) mice, and OVA-TcR tg mice (TcraTcrb, OT-I) mice were purchased from the Jackson Laboratory. *Csf2*$^{-/-}$ mice were provided by M. Manz (University Hospital, Zurich, Switzerland). B6.129S1-*Csf2rb*^{tm1Cgb}/J (*Csf2rb*$^{-/-}$) mice were provided by B. Becher (University Zürich). *Ccr2*$^{-/-}$ mice were maintained in our animal facility (Boring et al., 1997). *Csf1r*$^{fl/fl}$ mice were provided by J. Pollard (Li et al., 2006) (Albert Einstein, New York, NY). All animal procedures performed in this study were approved by the Institutional Animal Care and Use Committee (IACUC) of Mount Sinai School of Medicine.

Bone Marrow Chimeras

Bone marrow chimeras were generated as described previously (Ginhoux et al., 2009). In brief, $CD45.2^+$ WT mice were lethally irradiated (2× 550 rad, 3 hr apart by a Caesium source) and reconstituted with 5×10^6 BM cells of a 1:1 mixture of $CD45.1^+$ WT and $CD45.2^+$ WT or $CD45.1^+$ WT and $CD45.2^+$*Csf2rb*$^{-/-}$*Csf2rb2*$^{-/-}$ or $CD45.2^+$*Csf2rb*$^{-/-}$ BM cells or with 5×10^6 $CD45.1^+$ WT or $CD45.2^+$*Csf2rb*$^{-/-}$*Csf2rb2*$^{-/-}$ BM cells.

Cell Suspension Preparations

Cell suspensions were prepared as previously described (Ginhoux et al., 2009; Bogunovic et al., 2009) and analyzed by flow cytometry.

Flow Cytometry

Flow cytometry was performed with an LSR II (Becton Dickinson) and analyzed with FlowJo software (Tree Star). Fluorochrome- or biotin-conjugated monoclonal antibodies (mAbs) specific for mouse MHC class II I-A/I-E (clone M5/114.15.2), CD11b (clone M1/70), CD11c (clone N418), CD45 (clone 30-F11), CD45.1 (clone A20), CD45.2 (clone 104), CD115 (clone AFS98), Gr-1Ly6C/G (clone RB6-8C5), Ly6C (clone AL-21), Ly6G (clone 1A8), CD103 (clone 2E7), CD8α (clone 53-6.7), CD24 (clone M1/69), Mac-3 (clone M3/84), Sirpα (clone P84), Flt3 (Flk2) (clone A2F10), CD64 (X54-5/7.1), CD3 (145-2C11), B220 (clone RA3-6B2), TER-119 (TER-119), CD131 (clone JORO50), active Caspase-3 Ab (C92-605), and TNF-α (clone MP6-XT22) and the corresponding isotype controls and the secondary reagents were purchased either from BD Biosciences or eBioscience. CD123 mAb (clone 5B11) and CD125 mAb (clone T21) were purchased from Biolegend. F4/80 (A3-1) mAb was purchased from Serotec. Langerin Ab (clone E-17), donkey-anti-goat IgG-PE, and INOS Ab (clone M-19) were purchased from Santa Cruz. For intracellular TNF-α and iNOS staining, cells were incubated in vitro with brefeldin A for 4 hr at 37°C prior to intracellular staining according to the manufacturer's protocol. For Annexin-V staining (BD Biosciences), cells were stained with Annexin-V according to the manufacturer's protocol.

Gene Expression Profile

Single-cell suspensions of lymphoid and nonlymphoid tissues were prepared as described above. DCs were sorted on an ARIA sorter (BD). Microarray Affymetrix gene chip analysis of sorted monocytes, DC populations, and DC precursors were performed in collaboration with the Immunological Genome Project (Immgen).

Infections and Immunizations

Listeria monocytogenes—Mice were immunized i.v. with 2×10^4 CFU of *L. monocytogenes* 104035. On days 3 and 7 after infection, spleens and livers were removed and bacteria CFU was determined by plating serial dilutions of homogenized tissues on brain-heart infusion agar plates.

Influenza Virus—Influenza viruses (influenza strain A/Puerto Rico/8/34 (PR8) and influenza strain A/WSN/33 carrying chicken OVA peptide 257–264 SIINFEKL in the stalk region of neuraminidase (WSN:OTI) were grown either in 9-day-old embryonated eggs or in MDCK cells. Mice were infected i.n. with 10^4–10^7 PFU virus.

Streptococcus pneumoniae—Mice were inoculated i.n. with 10^6 CFU *S. pneumoniae* serotype 3 (ATCC 6303).

Lipopolysaccharide—Mice were injected i.v. with 20 μg of lipopolysaccharide (LPS) from *Escherichia coli* 0111:B4 (Sigma).

Salmonella Typhimurium—Infection with *S.* Typhimurium was described previously (Bogunovic et al., 2009). Mice were pretreated with 20 mg of streptomycin and 24 hr later, orally infected with 5×10^7 CFU of streptomycin-resistant WT *S.* Typhimurium.

Experimental Autoimmune Encephalitis—Mice were immunized s.c. in the lateral abdomen with 200 μg $MOG_{35–55}$ in CFA, and 200 ng pertussis toxin was administered i.p. on day 0 and day 2.

Monocyte Transfer

$Ly6C^{hi}$ monocytes were isolated as described previously (Ginhoux et al., 2006). In brief, monocytes were enriched with CD115-Biotin antibody and anti-Biotin microbeads (Miltenyi) and positively sorted by AutoMACS (Miltenyi). Subsequently, enriched monocytes were sorted ($DAPI^-CD3^-CD19^-Ly6G^-MHCII^-CD11c^-CD11b^+Ly6C^+F4/80^+CD115^+$) with an ARIA Sorter (BD). A 1:1 mixture of 6×10^6 WT (CD45.1) and 6×10^6 *Csf2rb*$^{-/-}$*Csf2rb2*$^{-/-}$ (CD45.2) monocytes was transferred into influenza-infected recipient mice.

Enzyme-Linked Immunosorbent Assay

Tissue samples were homogenized and lysed in lysing buffer (50 mM Tris, 5 mM EDTA, 150 mM NaCl, 1% NP40) containing proteinase inhibitors (Roche) for 30 min on ice. Protein concentrations were determined with a BCA protein assay kit (Pierce). ELISA for Csf-2 (eBioscence) and M-CSF (R&D) were performed according to the manufacturer's instructions.

Blocking Csf-1r Signaling In Vivo

Csf-1r mAb (clone AFS98) was purified from culture supernatant of AFS98 hybridoma (gift from S. Nishimura, New York) as previously described (Hashimoto et al., 2011a). Mice were injected i.p. at doses of 2 mg/mouse on day 0 and 1 mg/mouse on day 2.

Rosa26-CreER × *Csf1r*$^{fl/fl}$ mice were injected i.p. with 3.5 mg tamoxifen (Sigma T5648) dissolved in corn oil (Sigma) as previously described (Ginhoux et al., 2010).

Lung Immunization with OVA-Coated Beads

Mice were immunized with 50 µl of 1 µm latex beads (Polysciences) covalently coated with OVA (Sigma) according to the manufacturer's instructions and mixed with 10 µg of poly(I:C) prior to i.t. injection. For DC-OT-I T cell cultures, DC subsets were sorted from the lungs (3 hr postinjection) and lung-draining LN (24 and 72 hr postinjection) on an ARIA sorter (BD) and 10×10^3 DCs were cocultured with 100×10^3 OT-I CD8$^+$ T cells labeled with 5 µM CFSE (Molecular Probes).

Mitogreen and Anticleaved Caspase-3 Staining

DCs were sorted on an ARIA sorter (BD) and stained with 0.1 mM Mitogreen (Invitrogen) for 30 min at 37°C or with anticleaved Caspase-3 (Caltag) and counterstained with DAPI. Images were captured on a Zeiss Axio Imager Z1 with Axiocam MRM and were processed with Axiovision 4.8 Software.

In Vitro DC Culture

DCs were sorted as described above and cultured for 24 hr in the presence or absence of GM-CSF (50 ng/ml, Biolegend).

Statistical Analysis

Mean values, SEM values, and Student's t test (unpaired) were calculated with Prism (GraphPad software). *$p < 0.05$, **$p < 0.01$, ***$p < 0.001$.

Supplementary Material

Refer to Web version on PubMed Central for supplementary material.

Acknowledgments

We would like to thank B. Becher for critical discussions. B.D.B. is supported by JDRF172010770 and DP2DK083052-01. J.E.C. is supported by NIH CA157740 and 5-FY11-74 grant from the March of Dimes Foundation. E.L.G. is supported by American Heart Association Postdoctoral Fellowship (Founder's Affiliate). H.X. is supported by NIH R56AI091871 and the Eli and Edythe L. Broad Foundation. G.J.R. is supported by AI049653. J.W.P. is supported by R01 CA131270 and P01 CA100324. M.B. is supported by a career development award from the Crohn's and Colitis Foundation of America and a primary caregiver technical assistance supplement from the National Institute of Allergy and Infectious Diseases. M.G. is supported by the National Science Foundation of Switzerland. M.M. is supported by the National Institutes of Health grants HL086899, AI095611, and CA154947. P.S.F. is supported by HL69438, DK056638, HL097819, and HL097700.

REFERENCES

Aldridge JR Jr, Moseley CE, Boltz DA, Negovetich NJ, Reynolds C, Franks J, Brown SA, Doherty PC, Webster RG, Thomas PG. TNF/iNOS-producing dendritic cells are the necessary evil of lethal influenza virus infection. Proc. Natl. Acad. Sci. USA. 2009; 106:5306–5311. [PubMed: 19279209]

Bachem A, Güttler S, Hartung E, Ebstein F, Schaefer M, Tannert A, Salama A, Movassaghi K, Opitz C, Mages HW, et al. Superior antigen cross-presentation and XCR1 expression define human CD11c+CD141+ cells as homologues of mouse CD8+ dendritic cells. J. Exp. Med. 2010; 207:1273–1281. [PubMed: 20479115]

Banchereau J, Palucka AK. Dendritic cells as therapeutic vaccines against cancer. Nat. Rev. Immunol. 2005; 5:296–306. [PubMed: 15803149]

Bogunovic M, Ginhoux F, Helft J, Shang L, Hashimoto D, Greter M, Liu K, Jakubzick C, Ingersoll MA, Leboeuf M, et al. Origin of the lamina propria dendritic cell network. Immunity. 2009; 31:513–525. [PubMed: 19733489]

Boring L, Gosling J, Chensue SW, Kunkel SL, Farese RV Jr, Broxmeyer HE, Charo IF. Impaired monocyte migration and reduced type 1 (Th1) cytokine responses in C-C chemokine receptor 2 knockout mice. J. Clin. Invest. 1997; 100:2552–2561. [PubMed: 9366570]

Caux C, Vanbervliet B, Massacrier C, Dezutter-Dambuyant C, de Saint-Vis B, Jacquet C, Yoneda K, Imamura S, Schmitt D, Banchereau J. CD34+ hematopoietic progenitors from human cord blood differentiate along two independent dendritic cell pathways in response to GM-CSF+TNF alpha. J. Exp. Med. 1996; 184:695–706. [PubMed: 8760823]

Codarri L, Gyülvészi G, Tosevski V, Hesske L, Fontana A, Magnenat L, Suter T, Becher B. RORγt drives production of the cytokine GM-CSF in helper T cells, which is essential for the effector phase of autoimmune neuroinflammation. Nat. Immunol. 2011; 12:560–567. [PubMed: 21516112]

Crozat K, Guiton R, Contreras V, Feuillet V, Dutertre CA, Ventre E, Vu Manh TP, Baranek T, Storset AK, Marvel J, et al. The XC chemokine receptor 1 is a conserved selective marker of mammalian cells homologous to mouse CD8alpha+ dendritic cells. J. Exp. Med. 2010; 207:1283–1292. [PubMed: 20479118]

Dai XM, Ryan GR, Hapel AJ, Dominguez MG, Russell RG, Kapp S, Sylvestre V, Stanley ER. Targeted disruption of the mouse colony-stimulating factor 1 receptor gene results in osteopetrosis, mononuclear phagocyte deficiency, increased primitive progenitor cell frequencies, and reproductive defects. Blood. 2002; 99:111–120. [PubMed: 11756160]

Domínguez PM, Ardavín C. Differentiation and function of mouse monocyte-derived dendritic cells in steady state and inflammation. Immunol. Rev. 2010; 234:90–104. [PubMed: 20193014]

Dranoff G, Crawford AD, Sadelain M, Ream B, Rashid A, Bronson RT, Dickersin GR, Bachurski CJ, Mark EL, Whitsett JA, et al. Involvement of granulocyte-macrophage colony-stimulating factor in pulmonary homeostasis. Science. 1994; 264:713–716. [PubMed: 8171324]

Edelson BT, Kc W, Juang R, Kohyama M, Benoit LA, Klekotka PA, Moon C, Albring JC, Ise W, Michael DG, et al. Peripheral CD103+ dendritic cells form a unified subset developmentally related to CD8alpha+ conventional dendritic cells. J. Exp. Med. 2010; 207:823–836. [PubMed: 20351058]

Fogg DK, Sibon C, Miled C, Jung S, Aucouturier P, Littman DR, Cumano A, Geissmann F. A clonogenic bone marrow progenitor specific for macrophages and dendritic cells. Science. 2006; 311:83–87. [PubMed: 16322423]

Ginhoux F, Tacke F, Angeli V, Bogunovic M, Loubeau M, Dai XM, Stanley ER, Randolph GJ, Merad M. Langerhans cells arise from monocytes in vivo. Nat. Immunol. 2006; 7:265–273. [PubMed: 16444257]

Ginhoux F, Liu K, Helft J, Bogunovic M, Greter M, Hashimoto D, Price J, Yin N, Bromberg J, Lira SA, et al. The origin and development of nonlymphoid tissue CD103+ DCs. J. Exp. Med. 2009; 206:3115–3130. [PubMed: 20008528]

Ginhoux F, Greter M, Leboeuf M, Nandi S, See P, Gokhan S, Mehler MF, Conway SJ, Ng LG, Stanley ER, et al. Fate mapping analysis reveals that adult microglia derive from primitive macrophages. Science. 2010; 330:841–845. [PubMed: 20966214]

Guleria I, Pollard JW. Aberrant macrophage and neutrophil population dynamics and impaired Th1 response to *Listeria monocytogenes* in colony-stimulating factor 1-deficient mice. Infect. Immun. 2001; 69:1795–1807. [PubMed: 11179357]

Hamilton JA. Colony-stimulating factors in inflammation and autoimmunity. Nat. Rev. Immunol. 2008; 8:533–544. [PubMed: 18551128]

Hashimoto D, Chow A, Greter M, Saenger Y, Kwan WH, Leboeuf M, Ginhoux F, Ochando JC, Kunisaki Y, van Rooijen N, et al. Pretransplant CSF-1 therapy expands recipient macrophages and ameliorates GVHD after allogeneic hematopoietic cell transplantation. J. Exp. Med. 2011a; 208:1069–1082. [PubMed: 21536742]

Hashimoto D, Miller J, Merad M. Dendritic cell and macrophage heterogeneity in vivo. Immunity. 2011b; 35:323–335. [PubMed: 21943488]

Heath WR, Carbone FR. Dendritic cell subsets in primary and secondary T cell responses at body surfaces. Nat. Immunol. 2009; 10:1237–1244. [PubMed: 19915624]

Hildner K, Edelson BT, Purtha WE, Diamond M, Matsushita H, Kohyama M, Calderon B, Schraml BU, Unanue ER, Diamond MS, et al. Batf3 deficiency reveals a critical role for CD8alpha+ dendritic cells in cytotoxic T cell immunity. Science. 2008; 322:1097–1100. [PubMed: 19008445]

Inaba K, Inaba M, Romani N, Aya H, Deguchi M, Ikehara S, Muramatsu S, Steinman RM. Generation of large numbers of dendritic cells from mouse bone marrow cultures supplemented with granulocyte/macrophage colony-stimulating factor. J. Exp. Med. 1992; 176:1693–1702. [PubMed: 1460426]

Jakubzick C, Helft J, Kaplan TJ, Randolph GJ. Optimization of methods to study pulmonary dendritic cell migration reveals distinct capacities of DC subsets to acquire soluble versus particulate antigen. J. Immunol. Methods. 2008; 337:121–131. [PubMed: 18662693]

Jongbloed SL, Kassianos AJ, McDonald KJ, Clark GJ, Ju X, Angel CE, Chen CJ, Dunbar PR, Wadley RB, Jeet V, et al. Human CD141+ (BDCA-3)+ dendritic cells (DCs) represent a unique myeloid DC subset that cross-presents necrotic cell antigens. J. Exp. Med. 2010; 207:1247–1260. [PubMed: 20479116]

Karbowski M, Lee YJ, Gaume B, Jeong SY, Frank S, Nechushtan A, Santel A, Fuller M, Smith CL, Youle RJ. Spatial and temporal association of Bax with mitochondrial fission sites, Drp1, and Mfn2 during apoptosis. J. Cell Biol. 2002; 159:931–938. [PubMed: 12499352]

King IL, Kroenke MA, Segal BM. GM-CSF-dependent, CD103+ dermal dendritic cells play a critical role in Th effector cell differentiation after subcutaneous immunization. J. Exp. Med. 2010; 207:953–961. [PubMed: 20421390]

Kurihara T, Warr G, Loy J, Bravo R. Defects in macrophage recruitment and host defense in mice lacking the CCR2 chemokine receptor. J. Exp. Med. 1997; 186:1757–1762. [PubMed: 9362535]

León B, Ardavín C. Monocyte migration to inflamed skin and lymph nodes is differentially controlled by L-selectin and PSGL-1. Blood. 2008; 111:3126–3130. [PubMed: 18184867]

Li J, Chen K, Zhu L, Pollard JW. Conditional deletion of the colony stimulating factor-1 receptor (c-fms proto-oncogene) in mice. Genesis. 2006; 44:328–335. [PubMed: 16823860]

Liu K, Victora GD, Schwickert TA, Guermonprez P, Meredith MM, Yao K, Chu FF, Randolph GJ, Rudensky AY, Nussenzweig M. In vivo analysis of dendritic cell development and homeostasis. Science. 2009; 324:392–397. [PubMed: 19286519]

MacDonald KPA, Palmer JS, Cronau S, Seppanen E, Olver S, Raffelt NC, Kuns R, Pettit AR, Clouston A, Wainwright B, et al. An antibody against the colony-stimulating factor 1 receptor depletes the resident subset of monocytes and tissue- and tumor-associated macrophages but does not inhibit inflammation. Blood. 2010; 116:3955–3963. [PubMed: 20682855]

Martinez-Moczygemba M, Huston DP. Biology of common beta receptor-signaling cytokines: IL-3, IL-5, and GM-CSF. J. Allergy Clin. Immunol. 2003; 112:653–665. quiz 666. [PubMed: 14564341]

Martinou JC, Youle RJ. Mitochondria in apoptosis: Bcl-2 family members and mitochondrial dynamics. Dev. Cell. 2011; 21:92–101. [PubMed: 21763611]

Metcalf D. Hematopoietic cytokines. Blood. 2008; 111:485–491. [PubMed: 18182579]

Morrissey PJ, Bressler L, Park LS, Alpert A, Gillis S. Granulocyte-macrophage colony-stimulating factor augments the primary antibody response by enhancing the function of antigen-presenting cells. J. Immunol. 1987; 139:1113–1119. [PubMed: 3038997]

Naik SH, Metcalf D, van Nieuwenhuijze A, Wicks I, Wu L, O'Keeffe M, Shortman K. Intrasplenic steady-state dendritic cell precursors that are distinct from monocytes. Nat. Immunol. 2006; 7:663–671. [PubMed: 16680143]

Naik SH, Sathe P, Park HY, Metcalf D, Proietto AI, Dakic A, Carotta S, O'Keeffe M, Bahlo M, Papenfuss A, et al. Development of plasmacytoid and conventional dendritic cell subtypes from single precursor cells derived in vitro and in vivo. Nat. Immunol. 2007; 8:1217–1226. [PubMed: 17922015]

Nishinakamura R, Nakayama N, Hirabayashi Y, Inoue T, Aud D, McNeil T, Azuma S, Yoshida S, Toyoda Y, Arai K, et al. Mice deficient for the IL-3/GM-CSF/IL-5 beta c receptor exhibit lung pathology and impaired immune response, while beta IL3 receptor-deficient mice are normal. Immunity. 1995; 2:211–222. [PubMed: 7697542]

Onai N, Obata-Onai A, Schmid MA, Ohteki T, Jarrossay D, Manz MG. Identification of clonogenic common Flt3+M-CSFR+ plasmacytoid and conventional dendritic cell progenitors in mouse bone marrow. Nat. Immunol. 2007; 8:1207–1216. [PubMed: 17922016]

Poulin LF, Salio M, Griessinger E, Anjos-Afonso F, Craciun L, Chen JL, Keller AM, Joffre O, Zelenay S, Nye E, et al. Characterization of human DNGR-1+ BDCA3+ leukocytes as putative equivalents of mouse CD8alpha+ dendritic cells. J. Exp. Med. 2010; 207:1261–1271. [PubMed: 20479117]

Randolph GJ, Angeli V, Swartz MA. Dendritic-cell trafficking to lymph nodes through lymphatic vessels. Nat. Rev. Immunol. 2005; 5:617–628. [PubMed: 16056255]

Riedl SJ, Salvesen GS. The apoptosome: signalling platform of cell death. Nat. Rev. Mol. Cell Biol. 2007; 8:405–413. [PubMed: 17377525]

Robb L, Drinkwater CC, Metcalf D, Li R, Köntgen F, Nicola NA, Begley CG. Hematopoietic and lung abnormalities in mice with a null mutation of the common beta subunit of the receptors for granulocyte-macrophage colony-stimulating factor and interleukins 3 and 5. Proc. Natl. Acad. Sci. USA. 1995; 92:9565–9569. [PubMed: 7568173]

Rydström A, Wick MJ. Monocyte recruitment, activation, and function in the gut-associated lymphoid tissue during oral *Salmonella* infection. J. Immunol. 2007; 178:5789–5801. [PubMed: 17442963]

Sallusto F, Lanzavecchia A. Efficient presentation of soluble antigen by cultured human dendritic cells is maintained by granulocyte/macrophage colony-stimulating factor plus interleukin 4 and downregulated by tumor necrosis factor alpha. J. Exp. Med. 1994; 179:1109–1118. [PubMed: 8145033]

Sathe P, Pooley J, Vremec D, Mintern J, Jin JO, Wu L, Kwak JY, Villadangos JA, Shortman K. The acquisition of antigen cross-presentation function by newly formed dendritic cells. J. Immunol. 2011; 186:5184–5192. [PubMed: 21422244]

Schulz O, Jaensson E, Persson EK, Liu X, Worbs T, Agace WW, Pabst O. Intestinal CD103+, but not CX3CR1+, antigen sampling cells migrate in lymph and serve classical dendritic cell functions. J. Exp. Med. 2009; 206:3101–3114. [PubMed: 20008524]

Serbina NV, Salazar-Mather TP, Biron CA, Kuziel WA, Pamer EG. TNF/iNOS-producing dendritic cells mediate innate immune defense against bacterial infection. Immunity. 2003; 19:59–70. [PubMed: 12871639]

Serbina NV, Jia T, Hohl TM, Pamer EG. Monocyte-mediated defense against microbial pathogens. Annu. Rev. Immunol. 2008; 26:421–452. [PubMed: 18303997]

Shortman K, Naik SH. Steady-state and inflammatory dendritic-cell development. Nat. Rev. Immunol. 2007; 7:19–30. [PubMed: 17170756]

Sonderegger I, Iezzi G, Maier R, Schmitz N, Kurrer M, Kopf M. GM-CSF mediates autoimmunity by enhancing IL-6-dependent Th17 cell development and survival. J. Exp. Med. 2008; 205:2281–2294. [PubMed: 18779348]

Stanley E, Lieschke GJ, Grail D, Metcalf D, Hodgson G, Gall JA, Maher DW, Cebon J, Sinickas V, Dunn AR. Granulocyte/macrophage colony-stimulating factor-deficient mice show no major perturbation of hematopoiesis but develop a characteristic pulmonary pathology. Proc. Natl. Acad. Sci. USA. 1994; 91:5592–5596. [PubMed: 8202532]

Sudo T, Nishikawa S, Ogawa M, Kataoka H, Ohno N, Izawa A, Hayashi S, Nishikawa S. Functional hierarchy of c-kit and c-fms in intra-marrow production of CFU-M. Oncogene. 1995; 11:2469–2476. [PubMed: 8545103]

Trapnell BC, Whitsett JA, Nakata K. Pulmonary alveolar proteinosis. N. Engl. J. Med. 2003; 349:2527–2539. [PubMed: 14695413]

Varol C, Landsman L, Fogg DK, Greenshtein L, Gildor B, Margalit R, Kalchenko V, Geissmann F, Jung S. Monocytes give rise to mucosal, but not splenic, conventional dendritic cells. J. Exp. Med. 2007; 204:171–180. [PubMed: 17190836]

Varol C, Vallon-Eberhard A, Elinav E, Aychek T, Shapira Y, Luche H, Fehling HJ, Hardt WD, Shakhar G, Jung S. Intestinal lamina propria dendritic cell subsets have different origin and functions. Immunity. 2009; 31:502–512. [PubMed: 19733097]

Vremec D, Lieschke GJ, Dunn AR, Robb L, Metcalf D, Shortman K. The influence of granulocyte/macrophage colony-stimulating factor on dendritic cell levels in mouse lymphoid organs. Eur. J. Immunol. 1997; 27:40–44. [PubMed: 9021996]

Waskow C, Liu K, Darrasse-Jèze G, Guermonprez P, Ginhoux F, Merad M, Shengelia T, Yao K, Nussenzweig M. The receptor tyrosine kinase Flt3 is required for dendritic cell development in peripheral lymphoid tissues. Nat. Immunol. 2008; 9:676–683. [PubMed: 18469816]

Youle RJ, Karbowski M. Mitochondrial fission in apoptosis. Nat. Rev. Mol. Cell Biol. 2005; 6:657–663. [PubMed: 16025099]

Yu W, Chen J, Xiong Y, Pixley FJ, Dai XM, Yeung YG, Stanley ER. CSF-1 receptor structure/function in MacCsf1r−/− macrophages: regulation of proliferation, differentiation, and morphology. J. Leukoc. Biol. 2008; 84:852–863. [PubMed: 18519746]

Zhan Y, Carrington EM, van Nieuwenhuijze A, Bedoui S, Seah S, Xu Y, Wang N, Mintern JD, Villadangos JA, Wicks IP, Lew AM. GM-CSF increases cross-presentation and CD103 expression by mouse CD8+ spleen dendritic cells. Eur. J. Immunol. 2011; 41:2585–2595. [PubMed: 21660938]

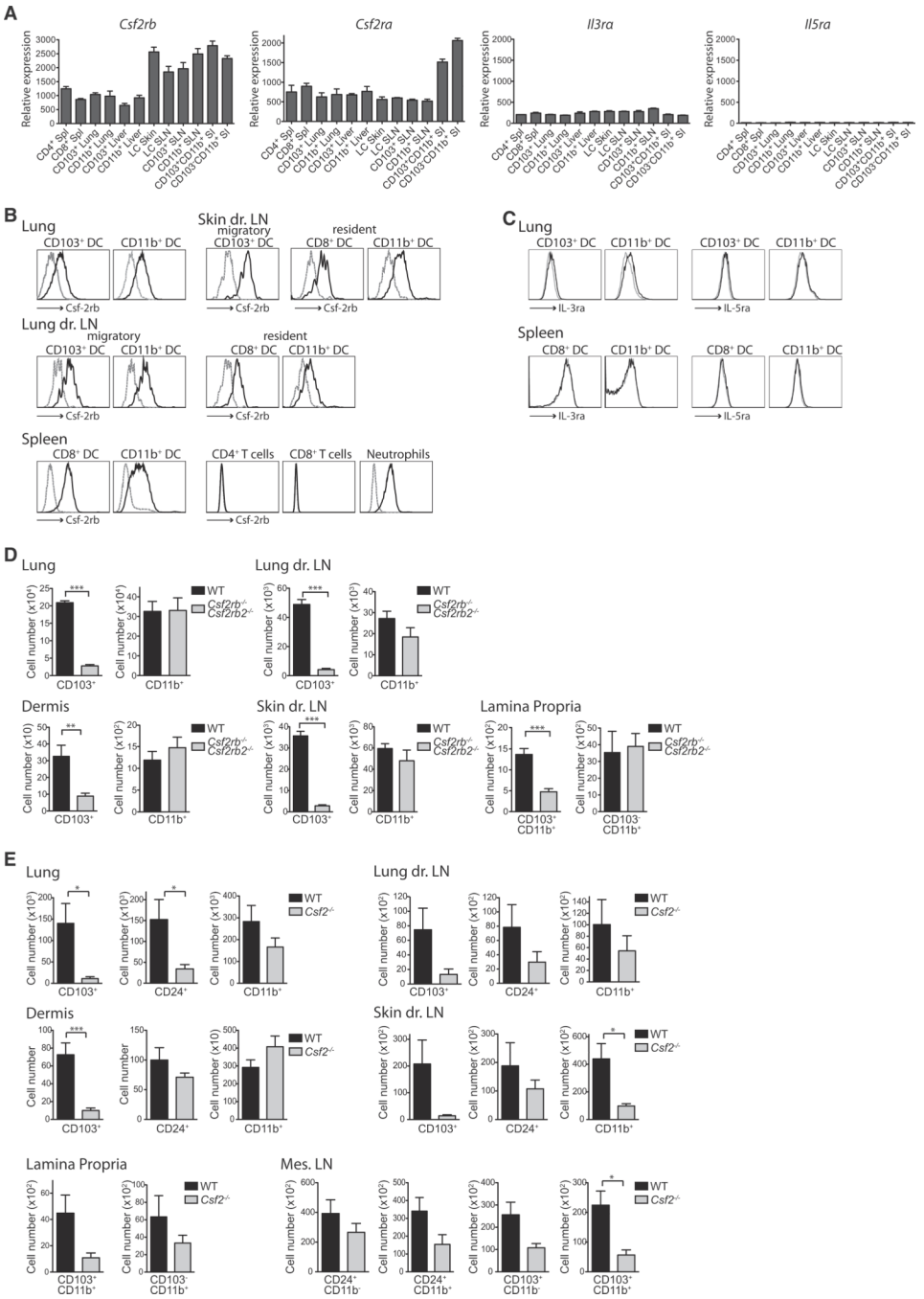

Figure 1. Csf-2r Is Highly Expressed on Nonlymphoid Tissue-Resident DCs in the Steady State

(A) *Csf2rb, Csf2ra, Il3ra*, and *Il5ra* expression profile of purified tissue DC populations was analyzed with Affymetrix gene chip arrays. Graphs show the relative mRNA expression of purified spleen-resident $CD8^+$ and $CD11b^+$ DCs, nonlymphoid tissue-resident $CD103^+$ and $CD11b^+$ DC subsets, migratory $CD103^+$ and $CD11b^+$ DCs in tissue-draining LNs, and epidermal and migratory LCs in skin-draining LNs isolated as described in Figure S1. Bar graphs represent the mean ± SEM ($n \geq 3$). Spl, spleen; SLN, skin-draining LN; SI, small intestine.

(B) Histograms depict the expression of Csf-2rb on DCs isolated from lymphoid and nonlymphoid tissues and $CD4^+$ ($CD4^+MHCII^-$) and $CD8^+$ ($CD8^+MHCII^-$) T cells and

neutrophils ($SSC^{hi}CD11b^{+}Gr1^{+}$) isolated from the spleen of WT mice. Dashed gray line, isotype control; solid black line, anti-Csf-2rb (CD131).
(C) Histograms depict the expression of IL-3ra and IL-5ra on DCs isolated from the spleen and lung of WT mice. Dashed gray line, isotype control; solid black line, IL-3ra (CD123) and IL-5ra (CD125) antibody.
(D and E) WT mice, *Csf2rb*$^{-/-}$*Csf2rb2*$^{-/-}$ mice (D), and *Csf2*$^{-/-}$ mice (E) were analyzed for the presence of the DC subsets as described in Figure S1A. Graphs show the absolute cell numbers of DCs in the lung (D and E: n = 6) and in the dermis (D and E: n ≥ 7), migratory DCs in skin-draining LNs (D and E: n = 4), lung-draining LNs (D and E: n = 4), and mesenteric (mes.) LNs (E: n = 3), and DCs in the lamina propria (D: n = 3, E: n = 4). Bar graphs represent the mean ± SEM.
*p < 0.05, **p < 0.01, ***p < 0.001 (Student's t test, unpaired).
See also Figure S2.

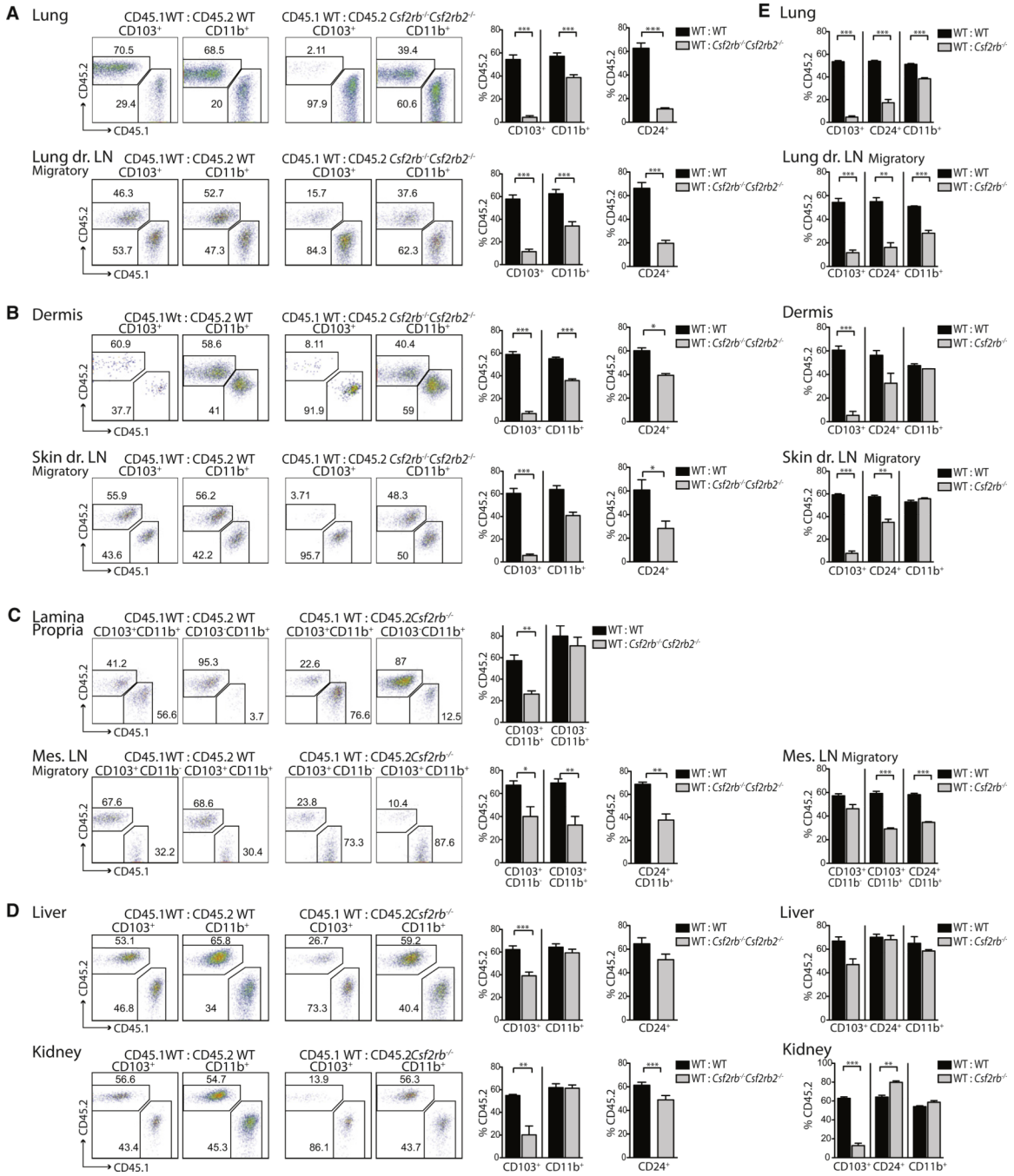

Figure 2. Csf-2r Controls the Development of Nonlymphoid Tissue DCs

Mixed BM chimeras (CD45.1$^+$ WT:CD45.2$^+$ WT and CD45.1$^+$ WT:CD45.2$^+$ *Csf2rb*$^{-/-}$ *Csf2rb2*$^{-/-}$ (A–D), CD45.1$^+$ WT:CD45.2$^+$ *Csf2rb*$^{-/-}$ (E)) were analyzed for the presence of CD45.1$^+$ and CD45.2$^+$ DCs. Dot plots show the percentage of CD45.1$^+$ WT and CD45.2$^+$ *Csf2rb*$^{-/-}$ *Csf2rb2*$^{-/-}$ nonlymphoid tissue-resident DCs and LN-migratory DCs as described in Figure S1A. Bar graphs display the percentage ± SEM of CD45.2$^+$ WT and CD45.2$^+$ *Csf2rb*$^{-/-}$ *Csf2rb2*$^{-/-}$ DCs (A–D) or CD45.2$^+$ *Csf2rb*$^{-/-}$ DCs (E). (A)–(D): Lung and lung-draining LNs, n = 6; skin-draining LNs, n = 7; dermis, n = 9; lamina propria and mesenteric LNs, n = 4; liver, n = 10; kidney, n = 4. (E): For all tissues, n = 3. *p < 0.05, **p < 0.01, ***p < 0.001 (Student's t test, unpaired).

See also Figure S3.

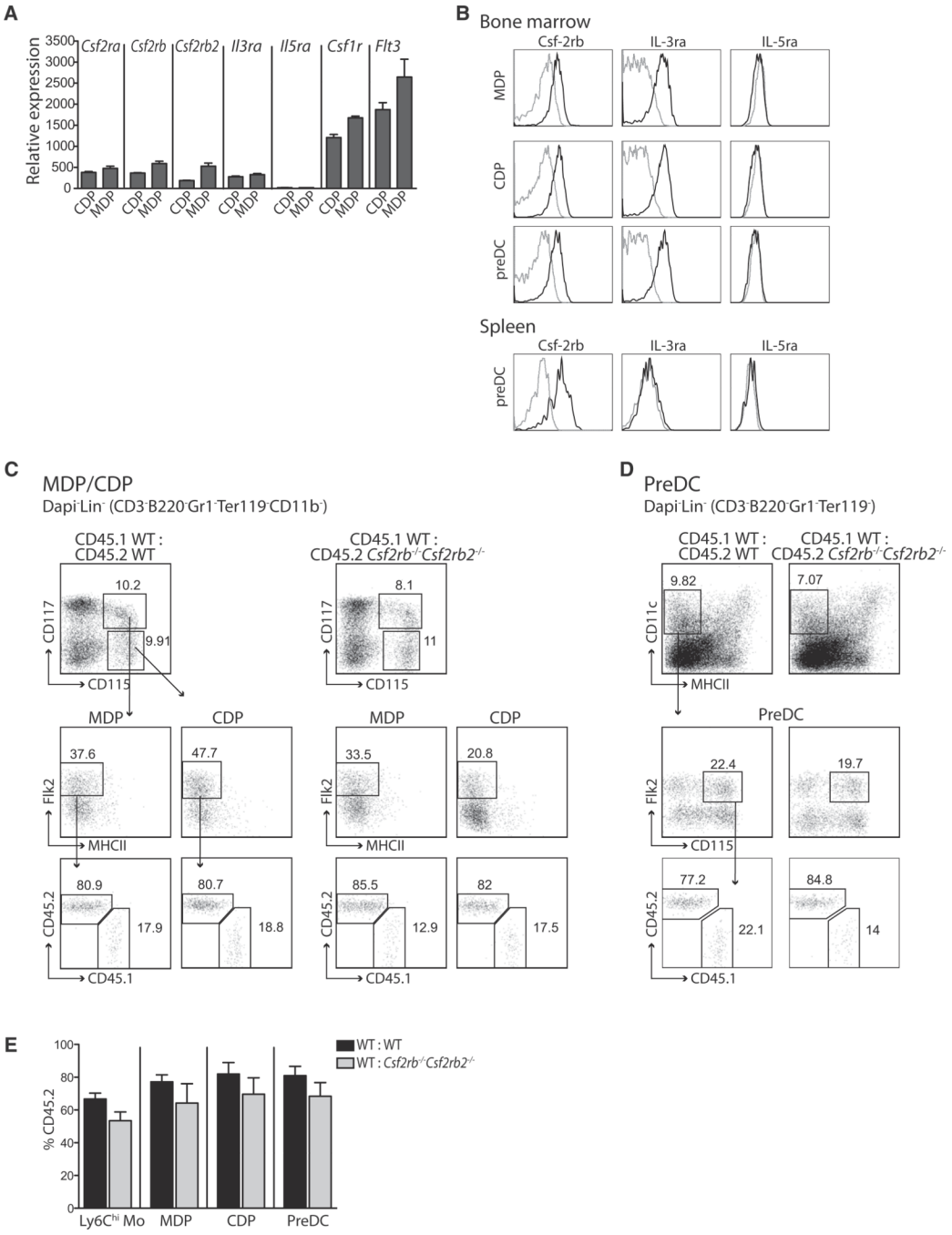

Figure 3. Csf-2r Does Not Control the Differentiation of DC-Restricted Precursors in the Bone Marrow

(A) *Csf2rb, Csf2rb2, Csf2ra, Il3ra, Il5ra, Csf1r*, and *Flt3* expression profile of purified precursor populations (CDPs and MDPs) from the BM of WT mice was analyzed with Affymetrix gene chip arrays. Graphs show the relative mRNA expression as the mean ± SEM (n ≥ 3).

(B) Histograms depict the expression of Csf-2rb, IL-3ra, and IL-5ra on MDPs, CDPs, and preDCs isolated from the BM and preDCs isolated from the spleen. Dashed gray line, isotype control; solid black line, antibodies against Csf-2rb, IL-3ra, and IL-5ra.

(C–E) Dot plots (C and D) depict the gating strategy to measure MDPs, CDPs (C), and preDCs (D) in the BM of mixed BM chimeras (CD45.1$^+$ WT:CD45.2$^+$ WT or CD45.1$^+$ WT:CD45.2$^+$ *Csf2rb*$^{-/-}$ *Csf2rb2*$^{-/-}$). Bar graphs (E) show the percentage ± SEM of CD45.2$^+$ circulating Ly6C^{hi} monocytes and BM preDCs, MDPs, and CDPs in mixed BM chimeric mice (n = 4).

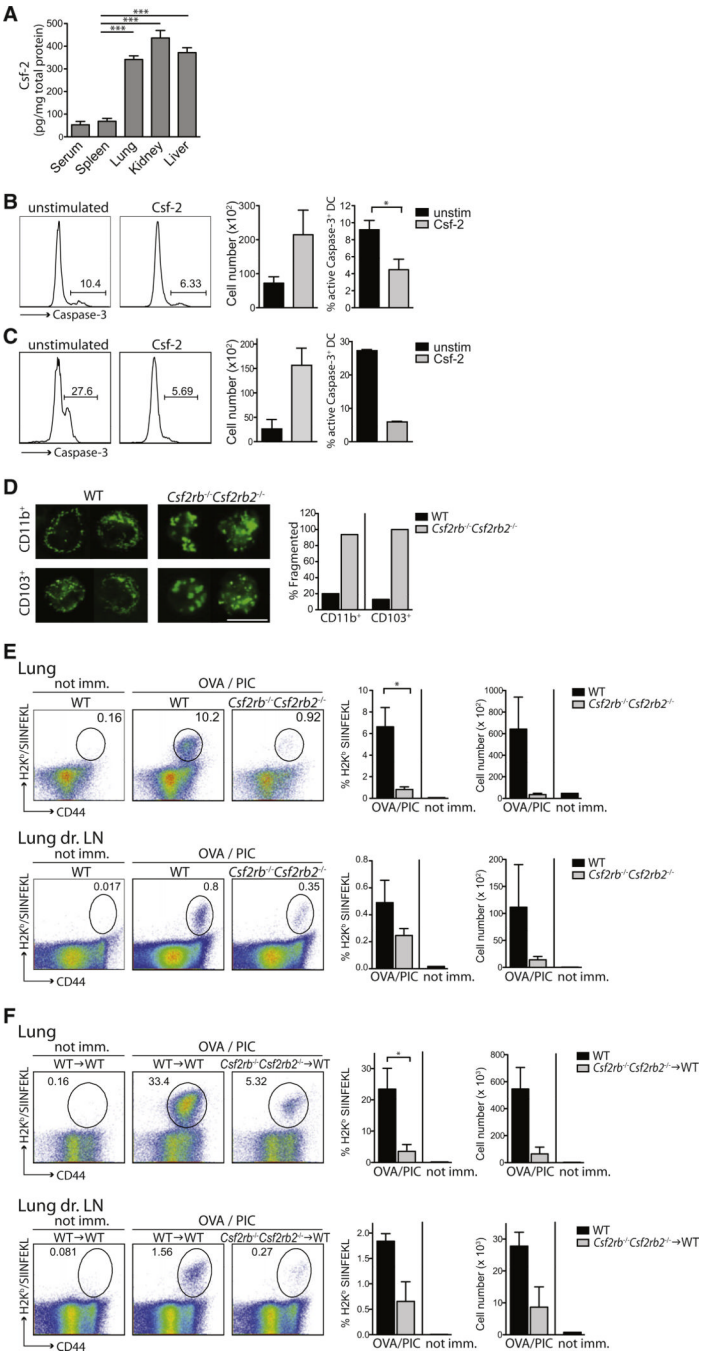

Figure 4. *Csf2rb*$^{-/-}$*Csf2rb2*$^{-/-}$ Mice Cannot Mount CD8^{+} T Cell Immunity upon Intratracheal Immunization with OVA Beads and Poly(I:C)

(A) Sera, lymphoid, and nonlymphoid tissues derived from naive WT mice were analyzed for Csf-2 levels by ELISA. Bars represent the mean ± SEM (n = 5).

(B and C) Splenic DCs (B) and lung CD103^{+} DCs (C) were isolated from WT animals and cultured for 24 hr with or without Csf-2. Plots show the percentage of active Caspase-3^{+} DCs and the total cell number of viable DCs (n ≥ 2).

(D) CD103^{+} and CD11b^{+} DCs were sorted from the lungs of CD45.1^{+} WT:CD45.2^{+} *Csf2rb*$^{-/-}$ *Csf2rb2*$^{-/-}$ BM chimeric mice and stained with Mitogreen. Images

show Mitogreen-stained DCs. Scale bar represents 10 μm. Bar graph depicts the percentage of DCs with fragmented mitochondria (n ≥ 100 cells).
(E and F) WT and *Csf2rb*$^{-/-}$*Csf2rb2*$^{-/-}$ mice (E) and WT and *Csf2rb*$^{-/-}$*Csf2rb2*$^{-/-}$ BM chimeric mice (WT→WT and *Csf2rb*$^{-/-}$→WT) (F) were immunized i.t. with OVA-coated latex beads mixed with poly(I:C) (OVA/PIC) or left untreated. 7 days after immunization, lungs and lung-draining LNs were analyzed for the presence of OVA-specific CD8$^+$ T cells via H2K^b/SIINFEKL-specific pentamers. Nonimmunized (not imm.) mice were used as controls. Plots represent the percentage and total cell number of OVA-specific CD8$^+$ T cells (gated on B220$^-$CD3$^+$CD8$^+$ cells) ± SEM (n = 3).
*p < 0.05, **p < 0.01, ***p < 0.001 (Student's t test, unpaired). See also Figures S4 and S5.

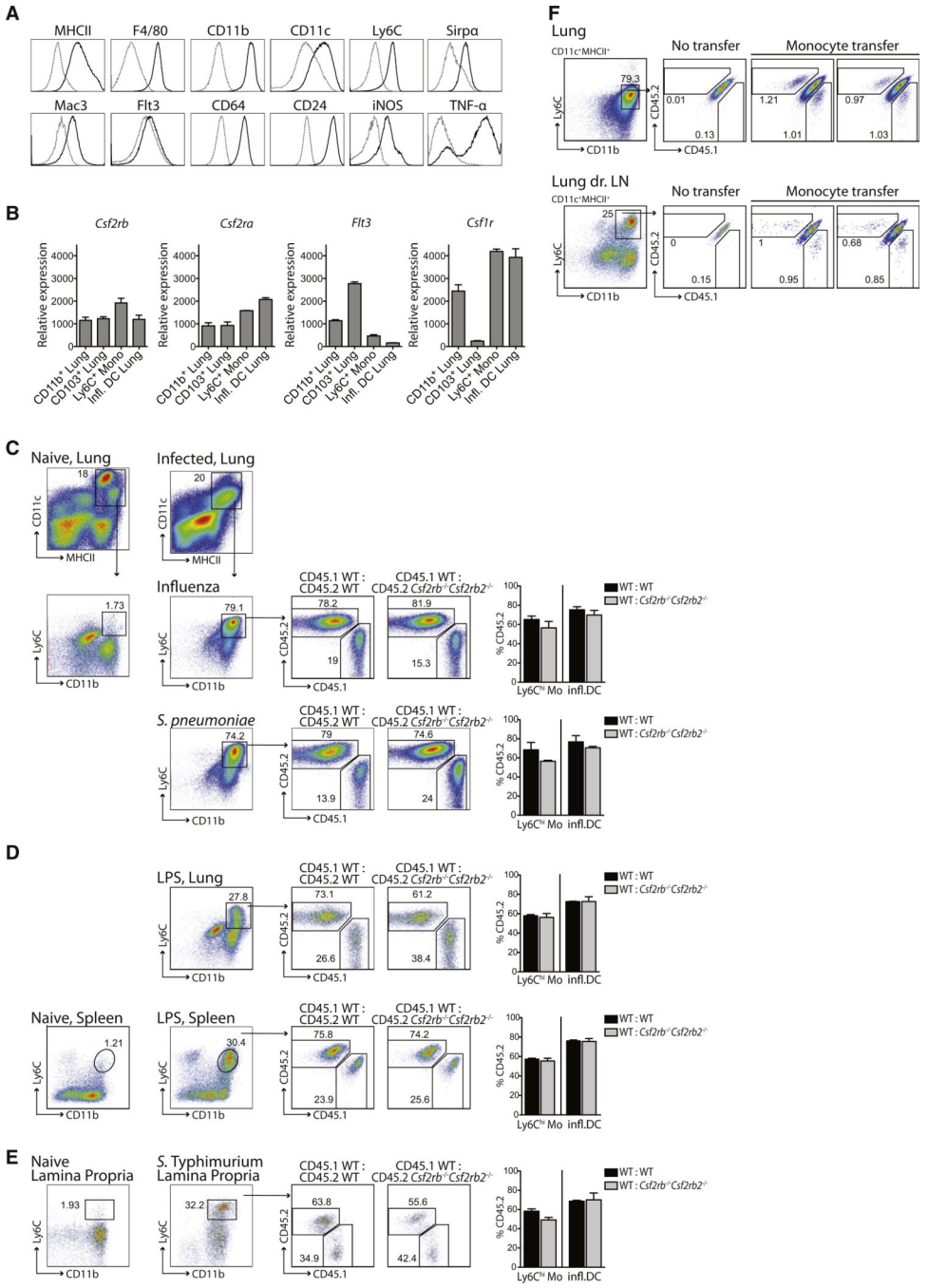

Figure 5. Inflammatory DCs Develop Independently of Csf-2r Signaling

(A) WT mice were inoculated i.n. with PR8 influenza virus. Histograms depict phenotypic analysis of inflammatory DCs that accumulate in the lungs on day 3 postinfection. Dashed gray line, isotype; solid black line, markers as indicated above the histograms.

(B) Graphs display *Csf2rb, Csf2ra, Flt3*, and *Csf1r* relative mRNA expression in naive WT Ly6C^{hi} blood monocytes, lung CD11b^{+} and CD103^{+} DCs isolated from naive WT mice, and inflammatory DCs (infl. DCs) isolated from the lungs of influenza virus-infected WT mice.

(C–E) Mixed BM chimeras (CD45.1^{+} WT:CD45.2^{+} WT or CD45.1^{+} WT:CD45.2^{+} *Csf2rb*$^{-/-}$ *Csf2rb2*$^{-/-}$) were either left untreated or submitted to infections or inflammation stimuli. Dot plots show the percentage of CD45.1^{+} WT,

CD45.2$^+$*Csf2rb*$^{-/-}$*Csf2rb2*$^{-/-}$, or CD45.2$^+$ WT DCs among total inflammatory DCs (DAPI$^-$CD11c$^+$MHCII$^+$CD11b$^+$Ly6C$^+$). Bar graphs display the percentage of CD45.2$^+$ inflammatory DCs of pooled experiments. As a reference population, circulating CD45.2$^+$ WT or *Csf2rb*$^{-/-}$*Csf2rb2*$^{-/-}$Ly6C^{hi} monocytes are shown.

(C) Mice were inoculated i.n. with influenza virus (n = 3) or *S. pneumoniae* (n = 4) and lungs were isolated 3 days later.

(D) Mice were injected with LPS i.v. and lungs and spleens were analyzed 24 hr later (n = 3).

(E) Mice were inoculated orally with *S.* Tymphimurium and lamina propria cells were analyzed 4 days later (n ≥ 3).

(F) Naive CD45.1$^+$CD45.2$^+$ F1 recipient mice were infected i.n. with influenza virus 24 hr prior to i.v. injection of a 1:1 mixture of CD45.1$^+$ WT:CD45.2$^+$*Csf2rb*$^{-/-}$*Csf2rb2*$^{-/-}$Ly6C^{hi} monocytes. Dot plots display the percentage of CD45.1$^+$ WT or CD45.2$^+$*Csf2rb*$^{-/-}$*Csf2rb2*$^{-/-}$ monocyte-derived inflammatory DCs (CD11c$^+$MHCII$^+$CD11b$^+$Ly6C$^+$) in the lungs and lung-draining LNs on day 3 after transfer. One representative of two independent experiments is shown.

See also Figure S6.

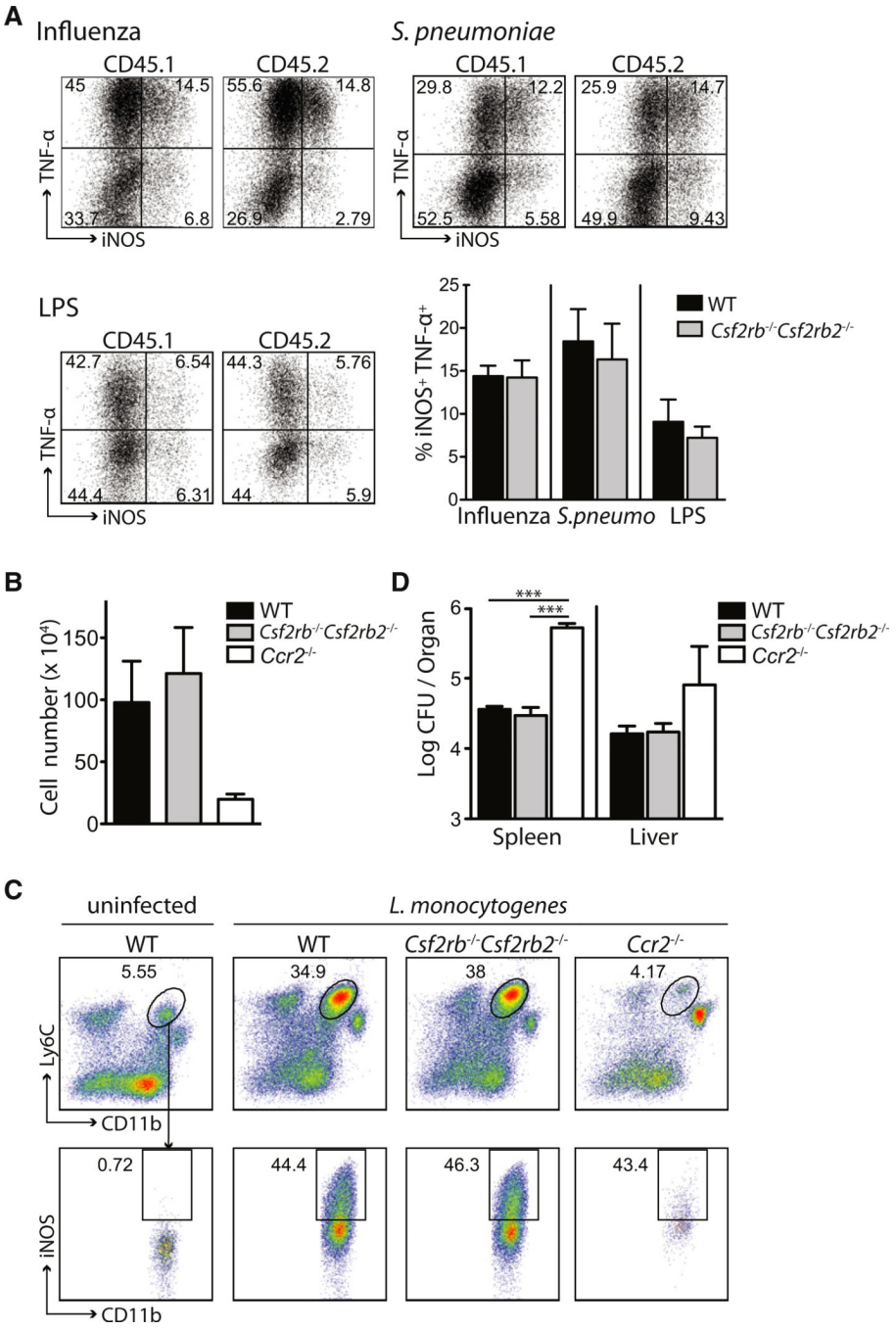

Figure 6. *Csf2rb*$^{-/-}$*Csf2rb2*$^{-/-}$ Inflammatory DCs Can Efficiently Control Initial *L. monocytogenes* Burden

(A) CD45.1^{+} WT:CD45.2^{+} *Csf2rb*$^{-/-}$ *Csf2rb2*$^{-/-}$ BM chimeras were infected i.n. with influenza virus (n = 3) or *S. pneumoniae* (n = 4) or injected with LPS i.v. (n = 3) as described in Figure 5. Graph and dot plots show the percentage of iNOS and TNF-α expression among CD45.1^{+} WT or CD45.2^{+} *Csf2rb*$^{-/-}$ *Csf2rb2*$^{-/-}$ inflammatory DCs (CD11c^{+}MHCII^{+}CD11b^{+}Ly6C^{+}) isolated from the infected lungs.

(B–D) WT, *Csf2rb*$^{-/-}$ *Csf2rb2*$^{-/-}$, and *Ccr2−/−* mice were inoculated i.p. with *L. monocytogenes*.

(B) Absolute cell number of inflammatory DCs gated on total DCs on day 3 postimmunization ± SEM (n = 4).
(C) Dot plots display the percentage of inflammatory DCs gated on total DCs ($CD11c^{+}MCHII^{+}$) and the percentage of inflammatory DCs expressing iNOS in the spleens of WT, *Csf2rb*$^{-/-}$*Csf2rb2*$^{-/-}$, and *Ccr2−/−* mice on day 3 after infection.
(D) Bar graph shows *L. monocytogenes* colony forming units (CFU) in the spleens and livers ± SEM (n = 4) on day 3 after infection. *p < 0.05, **p < 0.01, ***p < 0.001 (Student's t test, unpaired).

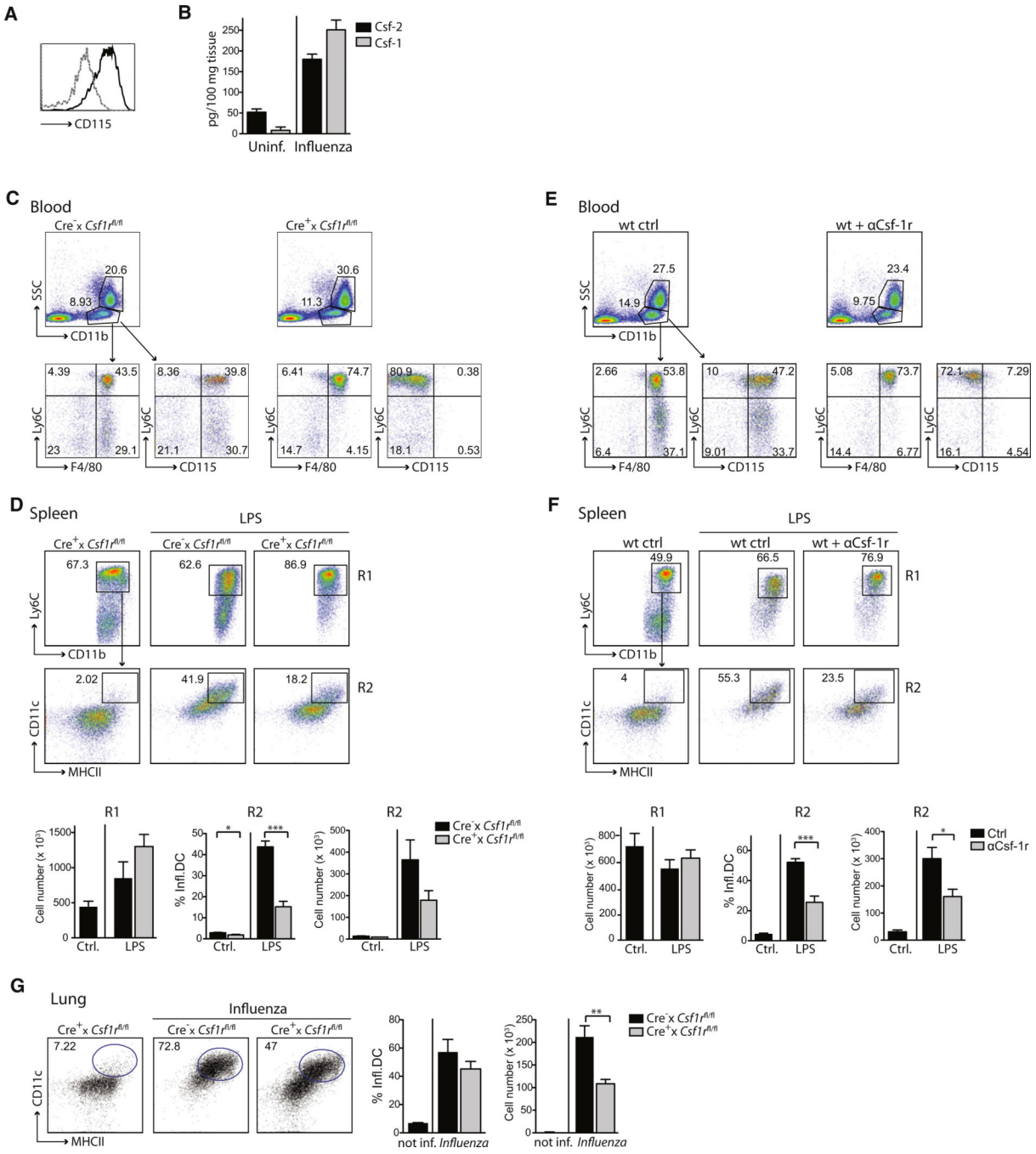

Figure 7. Csf-1r Signaling Controls the Development of Inflammatory DCs

(A) Histogram depicts CD115 expression of splenic inflammatory DCs isolated from LPS-treated WT mice. Dashed gray line, isotype control; solid black line, CD115 antibody.

(B) Lungs isolated from uninfected and influenza-infected WT mice were analyzed for Csf-1 and Csf-2 by ELISA (n = 3).

(C–F) Rosa26CreER^{+} (Cre^{+}) × *Csf1r*$^{fl/fl}$ and Rosa26CreER^{+} (Cre^{+}) × *Csf1r*$^{fl/fl}$ control mice were treated with tamoxifen (C, D) and WT mice were injected with Csf-1r antibody (αCsf-1r) (E, F). Seven days after treatment with tamoxifen or αCsf-1r, mice were injected i.v. with LPS.

(C and E) Dot plots display the percentage of $SSC^{lo}CD11b^{+}Ly6C^{+}$Csf-1r $(CD115)^{+}$ $F4/80^{+}$ circulating monocytes prior to LPS injection.
(D–F) Dot plots show the percentage of splenic monocytes (R1) ($DAPI^{-}Ly6G^{-}CD11b^{+}Ly6C^{+}F4/80^{+}$). R2 represents $MHCII^{+}CD11c^{+}$ DCs among gated R1 spleen monocytes. Graphs display the mean percentage and absolute cell number of spleen monocytes (R1) and inflammatory DC (R2) from combined experiments ± SEM on day 1 after LPS injection (n = 3 for controls [ctrl., no LPS], n = 6 for LPS-treated groups).
(G) Cre^{+} × *Csf1r*$^{fl/fl}$ and Cre^{-} × *Csf1r*$^{fl/fl}$ mice were treated with tamoxifen 14 days prior to being infected i.n. with influenza virus. Dot plots show the percentage and absolute cell number of lung inflammatory DCs ($DAPI^{-}CD45^{+}$Siglec-$F^{-}Ly6G^{-}CD11b^{+}F4/80^{+}$) 3 days after virus infection (n = 2 for control [not infected], n ≥ 4 for influenza virus-infected mice).
*p < 0.05, **p < 0.01, ***p < 0.001 (Student's t test, unpaired). See also Figure S7.